

NCRA Technical Report R233

September 3, 2008

Power-line Radio Frequency Interference at the GMRT

Govind Swarup, NCRA-TIFR, Pune, 411007

 NCRA-TIFR

Power-line Radio Frequency Interference at the GMRT

Table of Contents

Abstract

1. Introduction
2. Power-line RFI from Gap Discharges on the 11 kV lines
3. RFI from Corona Discharges on the Extra High voltage (EHV) lines such as 110 kV or 220 kV lines
4. Relation of Various Units Specified in the Literature for Measurements of Power Line RFI
5. Measurements of RFI at the GMRT in 1998 from Gap Discharges on the 11-kv lines
6. Measurements of Power-line RFI at the GMRT Antennas Made in 2003 and 2008
7. Comparison of Power-line Radio-Noise Reported in the Literature and Measurements Made at the GMRT
8. Minimizing RFI by Changing 11 kV Lines to 6 kV and or Using Fibre Glass Supports at the Electrical Poles
9. Identification of Defective Connections on the 11 kV and 33 kV lines
10. Location of Sources of Radio Noise from Power-lines near the Central Array Using the GMRT Array
11. A Mobile Van for monitoring RFI.
12. Electronic solutions
13. Mitigation Techniques to Minimize Harmful Affects of Power-line RFI during Calibration and Image-processing of the GMRT Observations.
14. Discussions, Recommendations and Conclusion
- 15. Acknowledgements:**
- 16. References**
- 17 Appendices** (copies of Appendices 1 to 5 available on request from gswarup29@gmail.com); A copy of Appendix A6 “A6. S. Pathak, G. Swarup A. Chatterjee and V. Kale, “Location of Radio Frequency Interference Using the GMRT”, given at the end of this report. The detailed procedure developed including software is available with Swarup.
- 18. Captions of 26 Figures and Table 1** (Figs and Table given in ITR-PL-Figs+T)

NCRA Technical Report ITR.....

Power-line Radio Frequency Interference at the GMRT

Govind Swarup, NCRA-TIFR, Pune, 411007

Abstract

High tension (H.T.) power-lines in the vicinity of the GMRT antennas produce harmful pulsed radio frequency interference (RFI) to radio astronomy observations, particularly in the 150 MHz band. Measurements show occurrence of groups of pulses occurring every 10 ms (half cycle of 50Hz), with each pulse of \approx tens to few hundred micro-second duration. The intensity of the pulses is often 10 or 20 dB above the system temperature of the GMRT receiver adversely affecting the achievable sensitivity of the GMRT at 150 MHz. Power-line RFI is also present at higher frequency bands of the GMRT but of lower intensity. The power flux density of the pulses decreases with increasing frequency as f^{-2} or f^{-3} , including consideration of the gain of the side-lobes of the primary antenna feed when it is pointed towards the dish. It would be interesting to estimate frequency dependence of the power-line RFI by taking Fourier transform of the pulsar observations at 150 MHz, 235 MHz and 325 MHz on a given day and finding the intensity of the 50 Hz pulses and of harmonics.

Measurements made by me and Raybole on 9th April 2008 indicate that the power- line RFI seems to be much higher now than that recorded by me in 1998 (we also found that the observed power-line RFI at the E2 antenna is extremely high, perhaps from the nearby 33 kV line needing an urgent correction). Although it would become possible to clip these sharp pulses at the input of the new software correlator, it is also important to carry out electrical and electronic solutions to minimize the power-line RFI, particularly for antennas of the Central Array of the GMRT. Clipping at the antennas is desirable in order to minimize any inter-modulation products due to the limited dynamic range of the laser diode of the optical fibre transmission system. This clipping at the antennas will be particularly important for the proposed 40MHz-60 MHz feed being developed by RRI for the GMRT.

It is known that severe radio noise (RFI) is generally caused by corona discharges on the HT lines of voltage > 65 kV. For lines of lower voltage, say of 11 kV and 33 kV, gap discharges at the insulators located at the electrical poles, poor grounding of the support arms and loose contacts in the joints gives rise to severe RFI. Similarly, RFI is also observed near the transformers of the irrigation pumps located near the antennas of the GMRT.

I describe in this report various solutions for minimizing power-line RFI at the GMRT antennas. These concern electrical, electronics and software solutions. I have incorporated some of the comments that I got when I gave a talk at GMRT on 10th April 2008. I summarize here some of my recommendations, supplementing the efforts being made by the GMRT group.

(a) Electrical solutions: Shri Swamy has tentatively proposed replacing the 11kV lines with the 6 kV lines. Swamy considers that using 11 kV insulators on the 6 kV line (and changing 11 kV/ 400 V transformers to 6kV/400V at each of the Y array antennas) may

offer higher resistance to the surface contaminants and any defects on the insulators that may result in lower RFI. It is not clear whether that would minimize power-line RFI appreciably since the gap discharge is a high impedance occurrence. Another proposal is to replace the metal support arms of the insulators at the electrical poles by fibre-glass arms. This proposal seems interesting and would be practical and economical if the fiberglass arms have sufficiently high impedance. One may also investigate insulators with semiconductor coating to minimize gap discharges as has been suggested in the literature. I would like to suggest that a temporary 11 kV line be constructed from the 2 MVA station of the GMRT to a distance of about 200m so that one could use it as test bed for investigating various solutions using good and defective insulators, fibre glass arms etc. It would also be worthwhile to consult experts at the Central Power Research Institute (CPRI) at Bangalore that has excellent high voltage test facilities. High voltage laboratory in the Indian Institute of Science at Bangalore has also experts and such facilities.

(b) Identification of defective connections on the 11 kV and 33 kV HT lines. GMRT staff is periodically locating defective connections and insulators on the electric poles of the HT lines and also loose connections at the irrigation pump transformers using an ultrasonic device, consisting of a small dish and an ultrasonic detector. Additionally, I would like to recommend building a compact portable battery operated amplifier with a gain of about 60 or 80 dB, with a small whip antenna at the input, a filter of about 1 MHz bandwidth. The amplifier may be tuned to a VHF frequency, say in between 60 or 70 MHz (where no strong CW signals may be seen at the GMRT). The output of the amplifier is to be connected to a diode detector followed by a sensitive 3 or 3½ digit voltmeter. This will provide quantitative measurements near the electric poles and as a function of distance. If an FM receiver is used, it would be important to add a RF amplifier of about 20 dB gain at the input to improve the sensitivity. Additionally, it would also be useful to suitably modify the software of the existing 30:1 RFI measurement set up, in order to allow zero 'span' observations remotely, including at Pune using our optical fibre link and also taking a Fourier Transform of the observed data in order to measure quantitatively values of the RFI. The GMRT group may also consider buying a standard radio noise measuring equipment using the European CISPR standard (it has also been adopted by the Indian Standard Institution, ISI).

(c) Electronic solutions: It is planned by the correlator group to clip the narrow pulses caused by power-lines using the new software correlator. The clipping may be done for a fraction of 1 ms whenever sharp pulses are detected with a time constant of about 50 microseconds at the input section of the software correlator (durations to be experimented). In my view it is important to clip the pulses at each antenna, just before the laser diodes of the optical fibre system, in order to avoid any inter-modulation products due to the limited dynamic range of only $\sim \pm 14$ dB of the laser diodes. This would also minimize RFI during thunderstorms. For pulsar observations or observations for celestial transient sources, such clipping would be disabled using the existing the Monitoring and Control Modules (MCM). Noise generator calibration would be required to measure the period for which the voltage signals are clipped in order to calibrate the gain of the antenna. I may add that observations in the frequency band of ~ 40 -60 MHz with the new feed being developed by

the Raman Research institute (RRI) for the GMRT are likely to be very seriously affected, unless sharp pulses of power-line RFI are clipped at each antenna.

(d) Software solutions: In addition to the clipping as described above, it should be possible to locate readily all the defective electrical poles and irrigation pump transformers, using a search technique similar to that developed by Pathak, Swarup, Chatterjee and Kale (2005). If differential GPS positions are determined for all the electric poles and irrigation pump transformers within a region of ~ 1 km surrounding the Central Array of the GMRT, it would be possible to locate harmful sources of power-line RFI expeditiously within \sim one hour (say every month) using the GMRT array electronics at ~ 150 MHz, with the present or new correlator system (though we should not wait for the new correlator). Thus MSEB can then take corrective steps readily within a few days in one go.

(e) This report is based on my personal understanding. I am aware that the GMRT group is already taking a number of steps to minimize power-line RFI to the GMRT. I wish them all success.

1. Introduction

The electrical power to the GMRT antennas is supplied by the Maharashtra State Electricity Board (MSEB) from a major sub-station located about 10 km south west from the Central array of the GMRT. The above MSEB sub-station is located about 3 km south of the town of Narayangaon. The Central array of the GMRT is located ~ 7 km north-east of the town of the Narayangaon. MSEB has constructed a special 33 kV line up to a 2MVA sub-station located at the north-western corner of the Central Array. From this sub-station an underground 11 kV cable runs to nearly a mid point of the Central array, where is located an 11 kV /400V 3 phase transformer, supplying power to all the 14 antennas of the Central Array and also to the laboratory building. Further, three 11 kV lines, each nearly 14 km long, have been constructed by the MSEB to supply electrical power to the western, eastern and southern arrays of the GMRT. A 110 kV line runs close to the E3 antenna, lying in between the E3 and E4 antennas. A few years ago, MSEB has constructed a 110 kV line passing nearly half-way in between W3 and W4 antennas. Figure S-1-1 gives a rough sketch of the above lines.

It is known that severe radio noise, giving Radio Frequency Interference (RFI), is caused by corona discharges on the lines of voltage > 65 kV. For lines of lower voltage, say of 11 and 33 kV, gap discharges at the insulators located at the electrical poles, poor grounding of the support arms and loose contacts in the joints can give rise to severe RFI. Similarly, RFI is also observed near the transformers of the irrigation pumps located near the antennas of the GMRT.

In Section 2, we summarize available literature concerning sources of radio noise (RFI) by gap discharges from high tension voltage lines of < 65 kV, resulting electric field strength, power flux density, expected frequency dependence and attenuation with distance. In Section 3, we summarize the same for RFI expected from the 110 kV line. Some of the important documents discussing the above dependence are attached as Appendices A1 to

A4. In Section 4 we have given relations between various units specified in the literature for measurements of the power line radio noise giving RFI

In Sections 5 and 6 are given power line radio noise (RFI) measured at the GMRT in 1998 and 2003 & 2008 respectively, from gap discharges on the 11-kV lines. In Section 7 are given a comparison between values of the power flux density of the power-line radio noise reported in the literature and that observed at the GMRT antennas.

We summarize in Sections 8 suggestions by the electrical group of the GMRT for minimizing RFI by electrical solutions. Appropriate surveys for identification of defective connections on the 11 kV and 33 kV lines are described in Section 9. In Section 10 we discuss an interesting scheme for location of sources of RFI by adding phases of the voltage signals of the Central Array antennas for determining location of any electric pole or transformer giving rise to RFI. Their positions are to be measured in advance using a GPS receiver. This scheme is extension of the work done by Pathak et al. (2005) at the GMRT in 2004. In Section 11 we discuss the importance of improving the existing mobile van for monitoring RFI not only from power-line RFI, but also that arising from the GMRT electronics, likely spurious emission from sources within ~ 30 km of the GMRT and unauthorized transmitters in the protected bands of the GMRT near Pune and surrounding regions. In Section 12 is discussed an electronics solution for clipping the pulses of the RFI at each antenna. In Section 13 we describe mitigation techniques being used by radio astronomers at NCRA for minimizing the harmful affects of the power-line RFI. Discussions, recommendations and conclusions are given in Section 14.

GMRT will certainly remain a dominant radio telescope in the world operating at meter and decimeter wavelengths for a long time. It is important and quite practical to minimize the harmful effects of the power-line RFI to the GMRT in order to achieve its theoretically expected high sensitivity at long wavelengths.

2. Power-line RFI from Gap Discharges on the 11 kV lines

Intensive radio noise (RFI) from the 11 kV power-lines is caused by gap-discharges due to large voltage gradients occurring across defective and/or contaminated insulators (by dust and impurities) and their rusted or loose supports on metal arms as well the poor grounding at the electric poles (Fig. S-2-1). Radiation arises due to avalanche chain reaction of electrons occurring across the gap (Skomel 1978). Alternating voltage of the 11 kV line gives rise to radiation at the fundamental frequency of 50 Hz and its harmonics from nonlinearities in the ionizing process. It may be noted that the frequency of electric supply sometimes varies in the range of ~ 48 to 52 Hz depending on the demand loads in the Pune region, though it is mostly near 50 Hz. The gap-discharge noise is likely to decrease in the presence of rains according to the literature but it is desirable to measure the same at the GMRT antennas. As shown in Fig. S-2.2, the radio noise by gap discharge was reduced by ~ 20 dB at frequencies $> \sim 10$ MHz. after repairs on the electrical poles. The gap discharge generally results in a series of several pulses occurring every ms apart or so, each being of few nanosecond (ns) duration. It gives rise to severe RFI in the VHF and UHF range. The frequency spectrum is also dependent on the radiation characteristic of the electric wires

next to the insulators and the supporting metal structure. Measurements have been made by several workers for the case of gap-discharges by relatively low voltage High Tension (H.T.) lines such as the 11 kV line and Extra-high voltage (EHV) H.T. lines of > 110 kV. The latter produces RFI mostly by corona discharges as discussed in Section 3, though the gap discharge noise may also be emitted for the EHV lines in case of faulty insulators or joints. The electric field strength varies as f^{-1} and the power flux density as f^{-2} (Figs.S-2-3; S-3-1, S-3-2, S-3-3 and S-3-4).

Assuming that gap discharge is initiated when the alternating voltage of the 11 kV lines exceeds say +5 kV and decreases to less than - 5 kV, we can predict the occurrence of the pulsed RFI to take place between $\sim \pm 5$ kV to nearly ± 11 kV, with respect to the zero voltage condition for all the 3 phases of the 11 kV supply (Fig.S-2-4). We will use these values in discussing observations of the GMRT antennas presented in Sections 5 and 6.

3. RFI from Corona discharges on the Extra High voltage (EHV) lines such as 110 kV or 220 kV lines

Unlike gap-discharge that takes place in the presence of two oppositely charged surfaces, corona discharge requires only a single charged surface at a sufficiently high potential. In case of AC lines, as the potential of the alternating voltage increases to a sufficiently high voltage (generally $> \sim 65$ kV), free electrons in the surrounding air are repelled for the negative cycle and are attracted towards the conductor for the positive cycle. The accelerated electrons impact molecules and give rise to a space charge in the vicinity of the conductor by the avalanche process. Corona is defined as “luminous discharge due to ionization of the air surrounding a conductor around which exist voltage gradient exceeding a certain critical value” (Pakala and Chartier 1971).

In contrast to the gap discharge, the corona discharge is not confined to the vicinity of the electrical poles and can take place anywhere on the conducting wires of the EHV line. The resulting electric pulse is generally of only a few ns duration but the radiated pulse width may also be dependent on the radiation characteristics of the long wires of the EHV lines. The measured frequency spectrum of the EHV lines varies as f^{-2} , as discussed below. Theoretical considerations and also measurements show that positive corona is of primary concern for the EHV lines and negative corona may be ignored (Skomel 1978; Pakala and Chartier 1971). Therefore we are not likely to see radio pulses every 10ms but only every 20 ms, in contrast to the 11 kV radio noise (to be verified by measurements at the GMRT for the E3 antenna in the vicinity of which a 110 kV lines is present). However, for the case of Corona discharge, it is likely that recurrent pulses may last for a longer time each cycle. Radio noise by the gap discharge is also known to occur in the EHV lines, such as 110 kV lines. It should be possible to minimize the Corona discharge by maintenance of the lines for a length of few km near the E3/E4 antennas and perhaps also replacing the present conductors with those of a larger diameter. According to the literature, radio noise from the corona discharge increases during rain.

I may add that radio noise due to the Corona discharge is also expected for the case of the 550 volt DC (HVDC) line running between the E5 and E6 antennas of the GMRT. The likely affect of the HVDC on the GMRT has been evaluated in detail by the well known expert, Mr Maruvada, from Canada who was entrusted consultancy by the MSEB. I plan to describe that study in another Internal Technical Report of NCRA.

In Fig.S-3-1 (inadvertently included twice in this ITR), are given spectra of the peak field strength of the radio noise from Corona discharge from a 244 kV AC transmission line, measured at distance of 200 ft. away (Pakala et. al. 1967; Fig. 3-16 of Skomel 1978). In a well cited paper, Pakala and Chartier have summarized radio noise measurements on overhead power lines from 2.4 kV to 800 kV (1971; Appendix A1). In Fig. S-3-2 we reproduce peak voltage measurements by Pakala and Chartier (1971, Fig. 10) of the frequency spectra for Corona discharge (fair weather) at 200 feet from the outside phase of 244, 345 and 735 kV lines. In Fig. S-3-3 are given plots of the noise factor F_a versus frequency for power lines from 12 kV to 230 kV, based on measurements made in the central Canada region (Bridges et al.1980: Fig. 1, Appendix A2).

In 1984, NRAO consulted V. L. Chartier to evaluate the likely RFI to the VLA from a 345 kV power line being planned by the El Paso Electric Co. running about 10 km from the VLA. The report by Chartier is reproduced by A. R. Thompson in the VLA Electronics Memorandum No. 211 (July 1984; our Appendix A3). Thomson has also summarized in his report the likely dependence of power flux density versus frequency and versus distance for a 362 kV line. As shown in Fig. 3-4, power line radio noise is expected to decrease in power as f^{-2} that is in agreement with f^{-1} dependence for the electric field strength as shown in Figs.S-2-3, S-3-1, S-3-2 and S-3-3. The dependence of the field strength ($20\log_{10} E/E_0$) varies as $1/d^3$, $1/d^2$, or $1/d$ depending upon the frequency and distance (Fig. S-3-6: Pakala and Chartier Figs 12, 13 and 14 and last line of their page 1162). For the GMRT frequencies we may use Fig.S-3-5, as given by Thompson. The attenuation of the signal depends not only on free space loss, that varies by $1/d^2$, but also on the heights of the transmitter and receiver above the earth (because the direct ray and that reflected by the earth may tend to cancel each other, resulting in larger attenuation compared to the free space attenuation). Since the primary feeds of the 45m dishes are at heights of ~ 30 to 45m above the earth (depending on their elevation values), we may consider attenuation to vary as $1/d^2$ for the power-lines located at distances of ~ 300 m to 700m, and $1/d^3$ for larger distances.

4. Relation of Various Units Specified in the Literature for Measurements of Power Line Radio Noise

Measurements of the electric field strength, E , of the radio noise is often specified in units of $\text{dB}\mu\text{V}/\text{m}/\text{MHz}$ or sometimes as $\text{dB}\mu\text{V}/\text{m}/120\text{kHz}$ (Figs S2-3, S3-1, S3-2, S3-3). Alternatively, values of the power flux density, P ($\text{dBW}/\text{m}^2/\text{MHz}$), of the radio noise are given by a factor, F_a , where $P = F_a \cdot k T_0 b$ ($k = 1.38 \times 10^{-23}$ Watts/Kelvin, $T_0 = 2900$ K and b is the bandwidth of the receiver). On the other hand, radio astronomers specify the received power flux density incident on an antenna in units of $\text{W}/\text{m}^2/\text{Hz}$, with $1 \text{ Jy} = 10^{-26} \text{ W}/\text{m}^2/\text{Hz}$. We may relate these units as follows:

Power flux density, $p = E^2 / Z_0$

where p is in units of $W/m^2/Hz$, E is in units of $V/m/Hz$ and the characteristics of the free space, $Z_0 = 377$ ohms. Hence, P (dBW/m²/MHz) = E^2 / Z_0 . If E is in units $1\mu V/m/MHz$, we get $P = 10 \log (10^{-12})/377 = -10 \log 2.6525 \times 10^{-15} = -145.76$ dB.

The peak values of the radio noise for a 4.6 kV line are $\sim (51 \pm 12)$ dB $\mu V/m/MHz$ at ~ 150 MHz at a distance of 50 feet (Fig.S-2-3). That corresponds to peak power flux density = $-145.76 + 51 = -94.76$ dBW/m²/MHz. In Section 6 is given a comparison of the measured values of RFI for the 11 kV and 110 kV power lines and those derived from the observations of RFI at the GMRT antennas.

5. Measurements of RFI made at the GMRT in 1998 from gap discharges on the 11-kv lines

5.1. 1998 observations: In this section are reproduce some of the measurements reported in the NCRA Internal Technical Report ITR R00186 by Swarup (2001). A few sentences from that report have been modified and significant changes are given in italics. The above ITR summarizes measurements made in 1998 of the broad-band pulsed interference due to the gap discharges in the 11 kV power-lines near the GMRT antennas as measured at the monitoring point soon after the output of the optical fibre in the receiver room of the GMRT. In Figs.S5-1 to S5-3 of the present report, are shown typical measurements made with the GMRT at 150, 235 and 327 MHz when the primary feeds are pointed towards the horizon in different directions. These measurements were done using the zero span mode of the HP-5890 Spectrum Analyzer (SpA), in which case the SpA acts as a receiver with the selected resolution bandwidth (RBW) of the SpA. The SpA was internally triggered by the 230 Volts single phase 50 Hz A.C. power. The value of the sweep (SWP) of the SpA was chosen as 20 or 40 milliseconds (ms). A video bandwidth of 100 kHz, corresponding to time constant of 10 micro-seconds (μs) was used. Since SpA measures values of the input power at ~ 400 points for each sweep, each point has duration of $\sim 50 \mu s$ for the 20ms sweep and $\sim 100 \mu s$ for the 40ms sweep. Measurements were made with the Resolution Bandwidth (RBW) of the SpA of 100 kHz, 1 MHz, 3 MHz and 5 MHz. It was generally found that the value of the power-line RFI was highest for a RBW of 3 MHz but more measurements are required to investigate this aspect. Also measurements need to be made for frequency dependence of the RFI as a function of bandwidth, BW, and observing frequency, f .

Figs. S5-1, S5-2, and S5-3 show that the pulsed radio noise (RFI) is ~ 20 dB above the receiver system noise ($= k.T_{sys}.b$) at 150 MHz and ~ 15 dB at 235 and ~ 10 dB at 325 MHz. Further, RFI occurs every 10 ms as discussed in Section II and sketched in Fig S2-4. In Fig.S5-1a, S5-1c and S5-2b, average of 100 scans was recorded, so that the power line RFI was averaged and only narrow band RFI by distant radio transmitters was seen.

In Figs. S5-4, S5-5, S5-6, 5-7 are shown measurements made at the baseband output of the C02 antenna (prior to the correlator input) using a battery operated digital oscilloscope. A diode detector followed by an integrator consisting of R and C with a time constant of 16

μs was placed at the baseband output. It is seen that the power line radio noise for each pulse rises in less than one μs (Fig. S5-5), has 1/e value of $\sim 50 \mu\text{s}$ (Fig. 5-4) and generally lasts for less than one ms (Figs. S5-1, S5-6, S6-1, S6-5). The intensity of the pulsed RFI varies considerably over several seconds as can be seen from Fig.S5-7 in which is presented observed RFI over a period of about 2.5 s. More measurements need to be made in this regard.

In Fig.S5-8 is shown a plot of the power spectrum of total power from one of the 45m antennas of the GMRT which was obtained by the Pulsar group with about time constant about 1 ms. It is seen that considerable power is observed at several harmonics of 50 Hz.

5.2. Line trigger observations (qs.: which of the 3 phases): As shown in Figs. S5-1 to S5-8, and in many observations made by radio astronomers, particularly in the 150 MHz band, a large degree of pulsed RFI is observed from the 11 kV power-lines located in the vicinity of the GMRT antennas. If RFI takes place due to the faulty insulators or poor junction connections or poor grounding at or a given pole of the 11 kV lines, we should expect RFI to occur when the amplitude of the A.C. voltage changes from $\sim \pm$ few kV (say ± 5 kV) to ± 11 kV. For the three phase lines which supply 11 kV power to the GMRT antennas, we should then expect to see pulsed RFI to arise at multiples of 3.33 ms for the 50 Hz frequency in India (Fig. 3-4). It is interesting to note that for most of the antennas of the GMRT, pulsed RFI was seen soon to arise after the line trigger of the SpA at either 3.3ms or 6.6ms or 10ms (starting often at 1ms or 2ms earlier to the above periods). Sometimes, RFI was observed only after every 20ms apart, indicating that gap discharge sparks occur only when the voltage changes from $\sim +5$ kV to $+ 11$ kV or ~ -5 kV to -11 kV and not for both cases. Thus it seems that the RFI arises mostly due to faulty connections or insulators and poor grounding at only one or two of the poles of the 11 kV power-lines, within a few hundred m of the GMRT antennas.

Recently it has also been found by M.R. Sankararaman and colleagues that there takes place considerable RFI from the 2-MVA sub-station supplying power to GMRT, which is located north-west corner of the Central Array of the GMRT, results for which will be described elsewhere. According to measurements made by me in 1998 and recently by Raybole and colleagues, it is found that the power-line RFI is also caused by the 11 kV power lines and transformer connections at the irrigation pumps in agricultural fields close to the GMRT antennas, perhaps up to several hundred meters away. In addition to the ultrasonic detector, we need to develop a hand-held RF measurement set up for measuring the amplitude of the power-line RFI from HT lines as discussed in Section 9.

6. Measurements of Power-line RFI at the GMRT Antennas Made in 2003 and 2008

In Figs.S6-1 to S6-4 are given power line RFI measured at 150 MHz by me and Raybole on Wednesday 09-April 2008 for ten GMRT antennas, viz. C0, C3, C8, C13, W2, W6, S1, S4, E2 and E5. At that time, the 610 MHz primary feeds were pointed towards the dishes and antennas were tracking 3C48. Therefore the 150 feeds were pointed towards the horizon. We requested GMRT operators to connect the 150 MHz feeds to the 150 amplifiers (using the usual control signal). Measurements were made in the receiver room at the monitoring

point just after the output of the optical fibre for each of the antennas using a spectrum analyzer with zero span option, RBW of 300 kHz, VBW of 100 kHz and sweep time of 20 ms. Over a period of about 30 seconds, several sweeps were made and generally a sweep with maximum RFI was saved. As can be seen, from the attached Figs., S6-2 to S6-6 that amplitude of the pulsed power line RFI exceeded 20 dB for many antennas. The power line RFI was seen to be worst for the E2 antenna (terrible indeed!) that arose most likely from the nearby 33 kV line. RFI was also found to be severe for the C13 and S1 antennas. Survey should also be done for other 20 antennas and particularly to investigate corona discharges by the 110kV line that passes between E3 and E4 antennas that may be producing large RFI in the rainy season.

Line trigger was used and therefore it was possible to make a guess regarding the phase of the 11kV lines near the GMRT antennas that gave rise to pulsed radio noise (RFI), using the Fig.S2-4. The concerned phase has been indicated by me on the margin of the plots of Figs.S5-1 to S5-3 and S6-1 to S6-6. Since pulsed RFI is often seen only for one of the 3 phases for many of the antennas, it indicates to me that the pulsed RFI arises often only from a single electric pole or an irrigation power transformer located near that antenna.

A 33 kV line lying only a few hundred m away from the northern boundary of the Central Array was constructed by the MSEB about 10 years ago as a standby line for their emergency use. It does not supply power to the GMRT except in the unlikely failure of power supply from the Narayangaon sub-station for an extended period. Since this line runs close to the Central Array, it produces additional power line RFI to the GMRT antennas apart from that caused by the 11 kV lines supplying power to the eastern and southern arrays, also located on the northern side of the Central Array. Since it is important to minimize RFI particularly to the Central Array, MSEB should be requested to disconnect this line (preferred) or charge it to 11kV. Nevertheless, the faulty insulators and loose connections on the 33 kV line within few hundred m of the E2 antenna need to be repaired with urgency.

7. Comparison of Power Line Radio-Noise Reported in the Literature and Measurements made at the GMRT

In this Section we compare values of power line radio noise (RFI) reported in the literature with those measured at the GMRT

7.1. Estimates of the power flux density by Nelson (1980) and Thompson (1984):

Nelson (1980) made an estimate of the likely interference to the Culgoora Radio Heliograph from a 132 kV line that was being planned by the NSW Electricity Commission in Australia and concluded that the line should be at least 5 km away from the telescope. Nelson considered the draft Australian Standard for 'Limits of Electromagnetic Interference from Overhead A.C. Power Lines' that sets limits to the RF interference in the frequency range 30 to 1000 MHz. According to the Australian Standard, electric field of the radio noise from the 132 kV line should not exceed +34 dB (= 2512) relative to $1\mu\text{V/m}/120\text{ kHz}$ bandwidth, at a location under the lines. Therefore, expected value of the power flux density, S , in units familiar to radio astronomers, under the line is as follows:

$$S = 2512 (E^2 / 377) / (120 \times 10^3) = 2512 (10^{-12} / 377) / (120 \times 10^3) = 5.55 \times 10^{-17} \text{ W m}^2 \text{ Hz}^{-1} = -162.6 \text{ dB W m}^{-2} \text{ Hz}^{-1}$$

Subtracting 10 dB for the expected attenuation from the EHV (A.C.) line to a point 200 feet away (Fig. 14 of Pakala and Chartier, 1971), reproduced by us as Fig. S3-6, we get S (200 feet.) = -172.6 dB W m⁻² Hz⁻¹. However, Thompson (1984, page 2 of his note: Appendix A1) has considered an attenuation of 20 dB from a distance of 10 feet to 200 feet, whence S (200 feet.) = -182.6 dB W m⁻² Hz⁻¹, close to the value of -188.5 dB W m⁻² Hz⁻¹ derived by Thompson (1984) for the rms value at 75 MHz for a distance of 200 feet. Thompson has summarized a report by the well known consultant V.L. Chartier recommending an acceptable distance of >7 km for the proposed 345 kV line from the Very Large Array (VLA) in New Mexico, U.S.A. Considering frequency dependence of f^{-2} , we subtract 6 dB from the 75 MHz value to derive the expected rms value of radio noise at 150 MHz from power lines at a distance of 200 feet, we get $S = -194.5 \text{ dB W m}^{-2} \text{ Hz}^{-1}$. Although this value is for EHV lines >110kV, we may also consider it for the 11kV and 33 kV lines (e.g. S3-3).

7.2. Measurements of radio noise from the power lines reported in the literature:

Values of radio noise from overhead power lines reported in the literature are based on CISPR standard applicable in Europe or ANSI in USA. Table 3.1 of Skomel (1978) gives a summary of the applicable charge time constant of 1 ms for both standards, but discharge time constant of 550 ms for the CISPR (15-300 MHz) and 600 ms for ANSI, as well some other characteristics. India also follows CISPR standard (IS 12233, Parts I, II and III). Commercially available equipment is used for these measurements.

In Table I we have summarized peak or quasi peak measurements reported in the literature for 1 MHz or 120 kHz bandwidths and then derived rms values of the power flux density, S , at 150 MHz at a distance of 200 feet. We have considered a difference of -10 dB for the rms values from the measured peak/quasi-peak values (Thompson 1984; Pakala and Chartier 1971) We have also made the required correction for the f^{-2} frequency dependence and dependence on the distance in order to estimate the radio noise values, S , at 150 MHz at a distance of 200 feet measured by a dipole at a height of 9 feet.

7.3. Summary of the measurements at the GMRT: It is difficult to estimate attenuation with distance from the 11 kV lines at heights from the ground of about 20 ft. (6 m) to the heights of the primary feeds of the GMRT antennas of ~ 130 feet (40 m). Nevertheless, we may use curves of Fig. S3-6 (Fig. 14 of Pakala and Chartier, 1971), (and Fig. S3-5 from Thompson), based on a height of 90 ft. for the electric line and 9 ft. for the dipole used for measurements. These values are approximately reverse of the GMRT case, with the heights of the 11 kV lines of ~ 20 feet (6m) and of the primary feeds of the GMRT antennas of ~ 130 feet (40m). A few of the GMRT antennas of the Central Array are located at a distance of only 600 ft. (~ 200 m) from the source of RFI, for which case the estimated additional attenuation from the 200 ft. values would be ~ -10 dB. However, many of the GMRT antennas of the Central Array are at a distance of ~ 2000 feet (600m) and the expected

attenuation may be ~ -25 dB. For the Y array antennas, attenuation values for 200 feet (60m) may be assumed.

The observed peak values of the pulsed RFI at the GMRT is about 20 dB above the noise of the receiver system $= kT_{\text{sys}} \cdot b$, where b is the bandwidth. We may assume the rms value of the power line RFI at the GMRT to be -20 dB compared to the peak values and thus the rms value is equal to $kT_{\text{sys}} \cdot b$ (it would be worthwhile to measure the rms value for several antennas with peak values of about 20 dB). Assuming attenuation of ~ 20 dB from 60m (200 feet) to the GMRT antennas at a distance of 600m and considering the area of the GMRT primary feed when pointed towards the horizon equal to a single dipole only (though its gain may be higher by a factor of ~ 4 when pointed towards the horizon), we estimate the rms value of the power flux density, S , received at the GMRT antennas at 150 MHz at 200 feet distance as follows:

$$S = (20\text{dB} + 20\log k T_{\text{sys}}) = -180 \text{ dB W m}^{-2} \text{ Hz}^{-1}.$$

This value is 14 dB higher than the value of $-194.1 \text{ dB W m}^{-2} \text{ Hz}^{-1}$ at 150 MHz at 200 feet estimated in Section 7.1 (see Table T1). As stated earlier, it is not straight forward to compare observed values at the GMRT with those in the literature. Nevertheless, it is clear from the measurements presented in Sections 5 and 6 that excessive pulsed RFI from power-lines is seen in the GMRT observations, which limits the achievable sensitivity of the GMRT, $= 50 \mu\text{Jy} = \sim -303\text{dB W m}^{-2} \text{ Hz}^{-1}$, after observations are made with all the 30 nos. of 45 m diameter antennas of the GMRT for 10 hours with the receiver bandwidth of 16 MHz, a remarkably low value of achievable flux density! As stated in the Introduction, it is important and quite practical to minimize the harmful effects of the power-line RFI to the GMRT, in order to achieve its expected high sensitivity at long wavelengths.

8. Minimizing RFI by Changing 11 kV Lines to 6 kV and or Using Fibre Glass Supports at the Electrical Poles

8.1 Fibre glass arms: Shri S. V. Swami, electrical engineer at the GMRT, and Shri N.V. Nagarathnam, Chief Engineer, have been considering various electrical solutions to minimize radio noise caused by gap discharges in the existing 11 kV lines supplying power to the GMRT (total length of ~ 50 km). Maintenance of these lines by replacing faulty insulators and loose connections has been quite cumbersome, with limited staff of MSEB and the lines falling in three different zones. It could be that gap discharges may be less for a 6 kV line with present 11 kV insulators but could still be significant. But 6 kV lines are not common in Maharashtra. A possible alternative is to use fibre glass arms instead of metal support arms but conductivity of these arms need to be considered as the gap discharge is a high impedance occurrence. Another suggestion in the literature is to use insulators at the electric poles coated by a suitable semi conductor to minimize charge build up. In order to investigate these possibilities, it is desirable to construct a dummy 3 phase 11 kV line from one of the 11 kV outputs of the 2 MVA transformer to a distance of about 200m so that one could use it as a test set up facility for mounting different insulators, with or without contaminants, or coated with semi-conductor and also fibre glass arms.

8.2. 33 kV and 11 kV lines: The radio noise from the two 11 kV lines located just north of the Central Array (supplying power to antennas of the eastern and southern arms of the Y-array), is likely to be correlated for several of the GMRT antennas of the Central Array. Hence, it would be important over the next couple of years (depending on the available budget) to lay an underground 11 kV line from the 2 MVA transformer at the Central Array to a point next to the C0 antenna, from where overhead lines may be connected for the above two arms. I had suggested the same in 1998 in a note to the late Vijay Kapahi. I may stress that it would not be possible to lay underground 11 kV cables for the Y array arms, as these lines pass through private fields. In principle the underground cables could be laid besides public roads, but the routes would be circuitous and the total length may exceed 60 km (> 80 crores!). Even then MSEB may not agree to do the same for the rural roads considering the safety aspects of the buried HT cables. Overhead 11 kV cables for a distance of ~ 500 m from each antenna (see Section 7.3 and next paragraph) could be useful. Further, the same would have to be done for any other 11 kV lines supplying power to the nearby villages and irrigation pumps if they pass close to the GMRT antennas. Hence we may confine to the above suggestions only for the Central Array.

To summarize: (a) The 33 kV line at the northern part of the GMRT antennas should be charged to only a few kV or should be diverted, (b) since the radio noise by power-lines is likely to be correlated for several of the GMRT antennas of the Central Array, it would be important to lay an underground 11 kV line from the 2 MVA transformer located at the north-west corner of the Central Array to a point next to the C0 antenna at the eastern end from where the overhead lines would be connected for the eastern and southern arms, and (c) further, it may be sufficient to carry out the above modifications for only 500m or 1 km from the GMRT antennas of the Y array antennas that should decrease the pulsed radio noise by at least 10 to 20 dB.

9. Identification of defective connections on the 11 kV and 33 kV lines.

At present the GMRT staff is periodically locating defective connections and insulators on the electric poles and connections near the irrigation pump transformers using an ultrasonic detector, consisting of a small dish and a detector. Additionally, I would like to stress the importance of building a compact portable battery operated amplifier with a gain of about 60 or 80 dB, with a small whip antenna at the input, and a filter of about 1 MHz bandwidth. The amplifier may be tuned to a frequency of 60 or 70 MHz (where no CW signals are seen at the GMRT). The output of the amplifier is to be connected to a diode detector followed by a sensitive 3 or 3½ digit voltmeter. This will provide quantitative measurements of the radio noise near the electric poles and as a function of distance. If an FM receiver is used, it would be important to add a RF amplifier of about 20 dB gain at the input to improve the sensitivity. Additionally, it would be useful to make additions to the software of the existing 30:1 RFI measurement set up, to allow zero 'span' observations remotely and also taking a Fourier Transform of the data to measure quantitatively value of the RFI, using a procedure adopted by the Pulsar group.

10. Location of Sources of Radio Noise from Power Lines near the Central Array using the GMRT Array

As discussed in this Section, it is quite practical to locate all or most of the sources of radio noise from power lines, say within a km or so of the Central Array, by using a similar method as described in a paper presented at the URSI General Assembly in New Delhi in 2005 by Pathak et al., entitled “Location of Radio Frequency Interference Using GMRT” (see Appendix A4). In that work position of a transmitter at a distance of about 5 km was determined by measuring phase of the received signals by the 12 antennas of the Central Array and using a search procedure that maximizes the value of the received signal as described below. I further suggest that positions of all the electrical poles and transformers within a km or so of the Central Array should be measured, using a GPS receiver (preferably a differential unit), so that the search can be speeded up and also false peaks of the expected side-lobes of the array towards the horizon can be avoided. It should be sufficient to make observations only for a few minutes, say 5 minutes, with the 150 MHz primary feeds of the GMRT dishes pointed towards the horizon and then antennas slewed by 90 degrees so that all the four directions are covered. An hour or so every month would provide information about all the sources giving rise to radio noise by gap-discharges. MSEB can then be requested to take corrective steps, within a few days, by their staff or an electrical contractor in collaboration with the GMRT. Thus, even the present correlator would be able to locate sources of the power line radio noise using a few minutes of observations. Further, the software correlator under development could be programmed to make the location expeditious but in my view we should not wait for that.

The method for locating sources of RFI using the central array antennas was developed during 2003-2004 by Sachin Pathak, Anirban Chatterjee and Vishal Kale, as part of their post-graduate projects with my close involvement. Procedure and software developed is described by Pathak in his M. Tech thesis, a copy available with me. Chatterjee made simulation for effective beam-width of the central array for a transmitter located ~ 10 km away. Swarup and Kale derived terrestrial geodetic coordinates (as are determined by the GPS) using the celestial coordinates of the GMRT antennas determined by Chengalur et al. based on astronomical observations. I give here a brief summary as described in the above cited paper: “we have used only 12 antennas of the central array located in a region of about 1 km x 1 km in extent. The primary feeds of the GMRT antennas placed near the focus have a 3dB HWFP of about 60 degrees. We rotate these feeds towards the horizon in specified directions. The voltage signals received by the feeds are cross-correlated using the electronic system of GMRT. The instrumental phase errors are calibrated by transmitting a signal from a signal generator located at a known position with respect to the array of GMRT. Procedure for data reduction and search for the location of an unknown transmitter and preliminary results are described in this paper. Our preliminary measurements show that it is possible to locate position of the unknown transmitter to an accuracy of less than 100 meter for distances of about 5 kilometer in a computer search time of about 100 s. It should be possible to extend the size of the array and use parallel processing computer for searching and locating RFI to much larger distances. The method developed may have wider applications in other communication systems”. The applicable equations are straight forward and can be provided by me.

11. A Mobile Van for monitoring RFI.

Considerable RFI is observed at the GMRT antennas not only by power lines but also by CW or narrow band signals at discrete frequencies (CW/NB) signals. Some of the NB signals are authorized signals in the region of about 30 km around the GMRT. However, many of the observed CW/NB signals are likely to be unauthorized signals or more likely spurious signals from mal-functioning equipment or from the GMRT electronics. Further many of the observed NB signals are likely to be unauthorized signals. It is desirable to locate such transmitters near the GMRT and also near Pune, particularly for the bands protected by the Government of India for radio astronomy so that no transmissions are permitted in these bands up to a distance of several hundred km from the GMRT. Letters of the concerned agencies of the Government of India are available in NCRA files.

I understand that a mobile van equipped with a log periodic antenna, RF amplifiers, spectrum analyzer and a diesel generator has been used occasionally for monitoring RFI near the vicinity of the GMRT antennas and particularly to locate mal-functioning (oscillating) booster-amplifiers that receive TV signals by residents in many villages. It would be desirable to improve this set up by adding a GPS receiver, a digital compass to find direction and a PC to record the output of the spectrum amplifier. A project student and a project technician could carry out the survey near all the GMRT antennas, and at several locations in a region of about 30 km of the GMRT to locate such transmitters. In 1998, a preliminary survey was carried out under my guidance at Pune, Lonavala, Junnar, near the GMRT antennas, Ale-Patha and Sangameer only in about a month using a simple set up as described in detail in Report 00191 (Swarup 2001). It is quite important to carry out these measurements again. Such a survey will supplement measurements made by Joardar and others at the GMRT.

12. Electronic solutions: It is planned to clip the received voltage from any of the GMRT antennas for a few hundred μ s (duration to be experimented), whenever sharp pulses are detected with a time constant of about 50 μ s at the input of the software correlator. The present laser diode at each antenna has a dynamic margin of only ~ 14 dB and hence large pulses of power-line RFI $> \sim 12$ dB are likely to produce non-linearity in the output of the laser diode of the optical fibre system, thus creating inter-modulation products, though of short duration. Therefore, it seems important to clip pulses of the power-line RFI at each antenna as described in Figure S-12-1. This scheme will also be useful for clipping narrow pulses observed during thunderstorms. For pulsar observations or observations for celestial transient sources, such clipping would be disabled. Noise generator calibration that is installed at each antenna but is not being used generally should be made available routinely and particularly to measure the period for which the voltage signals are clipped. The resulting data will be used for calibrating gain of the antenna every \sim one second.

13. Mitigation Techniques to Minimize Harmful Affects of Power-line RFI during Calibration and Image-processing of the GMRT Observations.

The Astronomical Image Processing Software (AIPS) allows clipping of the data for each of the multi-frequency channels or as a function of time and also above a certain rms value of the calibrated data. Since data is recorded generally every 16 s, it is not possible to clip sharp pulses of the power-line RFI. Sirothia has sometimes used data sampled every 128ms or 2s and used special procedure using AIPS++ to minimize the harmful affects of the power-line RFI and thus improve the achievable sensitivity of the GMRT. Recently Ramana Athreya has developed a special procedure for estimating the power-line RFI across the frequency band of 5.6 MHz at 235 MHz as part of the self-calibration procedure of the observations and thus has increased the dynamic range of the radio maps made by him, achieving $\sim 40000:1$ for observations near 3C286!. In Figure S13.1 is given a typical plot given to me by Ramana Athreya. It is interesting to note that his observations made with 4s integration gave rms variation of ~ 3 percent across the 5.6 MHz band at 235 MHz, more likely to arise from broadband power-line RFI.

14. Discussions, Recommendations and Conclusion

High tension (H.T.) power-lines near the GMRT antennas give rise to pulsed radio frequency interference (RFI) to the radio astronomy observations, particularly for the 150 MHz band. Pulsed power-line RFI is also observed in the 235MHz and 325 MHz band. Measurements show occurrence of groups of pulses occurring every 10 ms (half cycle of 50Hz), with each pulse of duration of \sim tens to few hundred micro-second. The intensity of the pulses is often seen as 10 or 20 dB above the system temperature of the GMRT receivers, adversely affecting the achievable sensitivity of the GMRT at 150 MHz.

In Sections 5 to 8 we have summarized expected value of the power-flux density from the literature and compared with measurements made at the GMRT. Since measurements have been made with different apparatus and at different distances, it was not possible to make clear conclusions. Nevertheless, GMRT measurements presented in Sections 5 and 6, as well analysis of observations by several workers (e.g. Athrey, Sirothia and others) make it quite clear that the RFI by 11 kV lines adversely affects the GMRT sensitivity, particularly at 150 MHz. A. P. Rao has told me that there seems to be present broadband RFI in the GMRT observations. Recent observations by Syed Ali and Chengalur at 150 MHz also show likely presence of broad band noise. I consider that correlated broadband RFI arises from the 11 kV power-lines, particularly for observations made with the Central Array antennas. Observations in the frequency band of ~ 40 -60 MHz with the new feed being developed by the Raman Research institute (RRI) would be affected very adversely unless clipping is done of the sharp pulses of the power-line RFI at each antenna.

Line trigger was used by me for observations described in Sections 5 and 6. This procedure made it possible for me to make a guess regarding the phase of the 11kV lines near the GMRT antennas that gave rise to pulsed radio noise (RFI), using the Fig. 2-4. The concerned phase has been indicated by me on the margin of the plots of Figs.S5-1 to S5-3 and S6-1 to S6-6. Since notable pulsed RFI is generally seen only for one phase in the case of several antennas, it indicates that the source of severe RFI is likely to arise from only one electric pole or an irrigation power transformer located near these antennas. Hence, as

discussed in Section 8, it could be sufficient to improve the 11 kV lines within a km from the edges of the Central Array and ~ 600 m from each of the antennas of the Y array.

Power-line RFI is also present in the higher frequency bands of the GMRT but of lower intensity. As suggested in this report, it is likely to be proportional to f^{-2} or f^{-3} , as received by the side-lobes of the primary antenna feed when it is pointed towards the dish. It would be interesting to estimate frequency dependence of the power-line RFI by taking Fourier transform of the pulsar observations at 150 MHz, 235 MHz and 325 MHz on a given day and finding the intensity of the 50 Hz pulses and of harmonics.

Measurements made by me and Raybole on 9th April 2008 indicate that the power-line RFI seems to be much higher now than that recorded by me in 1998 and by others in 2003. Although it would become possible to clip the sharp pulses at the input of the new software correlator, it is also important to carry out electrical and electronic solutions to minimize the power-line RFI, particularly for antennas of the Central Array of the GMRT.

I summarize here some of the major recommendations. I understand that some of the suggested modifications are already planned by the GMRT group:

(a) Electrical solutions: I would like to suggest that a temporary 11 kV line be constructed from the 2 MVA station of the GMRT to a distance of about 200m so that one could use it as test bed for investigating various solutions, using good and defective insulators, fibre glass arms etc.

(b) Identification of defective connections on the 11 kV and 33 kV lines. Survey is being done by the GMRT staff using an ultrasonic detector, consisting of a small parabolic dish of ~ 500 m diameter and an ultrasonic detector. Additionally, it is important to build a compact portable battery operated amplifier with a gain of about 60 or 80 dB at a suitable frequency in the range of 60 to 70 MHz (where no strong RF signal is observed), with a small whip antenna at the input, a filter of about 1 MHz bandwidth and connected to a diode detector followed by a sensitive 3 or 3½ digit voltmeter. This will provide quantitative measurements near the electric poles and as a function of distance. Additionally, it would also be useful to make additions to the software of the existing 30:1 RFI measurement set up, to allow zero 'span' observations remotely as well taking a Fourier Transform to measure quantitatively value of the RFI.

(c) Electronic solutions: Although it should be possible to clip the received voltage from any of the GMRT antennas for a few hundred microseconds (duration to be experimented), whenever sharp pulses are detected with a time constant of about tens of microseconds at the input section of the software correlator, it is also desirable to similarly clip the data at each antenna as discussed in this report so that non-linearity of the laser diode at the antennas do not give rise to harmonics of RFI. This scheme will also allow clipping of thunderstorm created pulses. Of-course, for pulsar observations or observations for celestial transient sources, such clipping would be disabled. Noise generator calibration would be needed to measure the period over which the received voltage signals are clipped and the data used to calibrate the gain of the antenna. I may add that observations planned with the

GMRT in the frequency band of ~ 40-60 MHz with the new feed being developed by the Raman Research institute (RRI) would be very seriously affected unless clipping is done of sharp pulses at each antenna.

(d) Software solutions: In addition to the clipping as described above, it should be possible to locate all the defective electrical poles and irrigation pump transformers, using a search technique similar to that developed by Pathak, Swarup, Chatterjee and Kale (2005). All the 150 MHz primary feeds of the Central Array antennas of the GMRT were pointed by them to the West. GMRT electronics was calibrated using AIPS. Pathak et al. searched over a wide region to locate a transmitter placed at an unknown position about 5 km away from the GMRT and located it to an accuracy <100 m. Further, I suggest that differential GPS positions should be measured for all the electric poles and irrigation pump transformers within a km of the Central Array that would allow locating sources of power-line RFI expeditiously. An hour or so every month would provide information about all the sources giving rise to radio noise by gap-discharges. MSEB can then be requested to take corrective steps, within a few days, by their staff or an electrical contractor in collaboration with the GMRT. Even the present correlator would be able to locate sources of the power line radio noise using a few minutes of observations. Further, the software correlator under development could be programmed to make the location expeditious but in my view we should not wait for that.

It may be not out of place here to state that there was only one two-story building at Narayangaon when we decided to select the present location for the GMRT. Now there are hundreds! We did not consider the likely explosion of population in the region as a result of new irrigation dams being constructed. We also did not anticipate northward industrial expansion from the city of Pune towards Rajgurunagar (although we were forewarned about that likely occurrence by the late Dr. Raja Ramanna in 1986). Considerable RFI is consequently observed at the GMRT site, but various mitigation techniques should minimize, though not eliminate its harmful affects.

GMRT will certainly remain a dominant radio telescope in the world operating at meter and decimeter wavelengths for a long time. It is very important and quite practical to minimize the harmful effects of the power-line RFI to the GMRT in order to achieve close to its expected theoretical high sensitivity at long wavelengths.

15. Acknowledgements

I thank several engineers and technical persons for their valuable comments made during my talk on the subject at the GMRT on 10th April 2008. I also thank Sandeep Sirothia for many discussions and Ramana Athreya for Fig.S13.1.

16. References

E. Bridges, E., Goddard, W.R., Gad, T. and Boerner, W.M., "Measurement and Study of Radio Noise from Power lines in the Central Canada Region", IEEE, 1980, (CH-1538-8/80/0000-0021 \$00.75), pp. 21-25.

Nelson,G.J.,“Proposed 132 kV Transmission Line near Culgoora” 28 may 1980, 7 pages.

Pakala, P.E. and Chartier, V.L., “Radio Noise Measurement on overhead power lines from 2.4 to 800 kV”, IEEE Transactions on Power Apparatus and Systems, Vol. PAS-90, No. 3, May-June 1971, pp. 1155-1165.

S. Pathak,S., G. Swarup,G., Chatterjee,A. and Kale, V., “Location of Radio Frequency Interference Using the GMRT”, paper presented at the General assembly of the International Radio Scientific Union, held at New Delhi, November 2005.

Skomel, E N, “Man Made Radio Noise” Pub., Van Nostrand Reinhold, 1978, pp. 342.

Swarup,G., ‘Radio Frequency Coordination, Interference Measurements, and Mitigation Techniques Regarding the Giant Metrewave Radio Telescope’. NCRA/TIFR, Pune 411007, Internal Technical Report R00186, Part I, 2001, pp. ---.

Swarup, G., “Surveys of Radio Frequency Interference (RFI) at the GMRT SITE from Terrestrial Transmitters:, NCRA,TIFR, Internal Technical Report,R00191, Part IV, 2001, pp.---.

A.R. Thompson, A.R., “Radio Interference from High-Voltage Power Lines”, VLA Electronics Memorandum No. 211, July 1984 discussing RFI protection of the VLA at 75 MHz from a 110 kV line (including two appendices by V.L. Chartier).

Appendices

A1. A.R. Thompson, “Radio Interference from High-Voltage Power Lines”: VLA Electronics Memorandum No. 211, July 1984, discussing RFI protection of the VLA at 75 MHz from a 110 kV line (including two appendices by V.L. Chartier).

A2. W.E. Pakala and V.L. Chartier: “Radio Noise Measurement on overhead power lines from 2.4 to 800 kV”, IEEE Transactions on Power Apparatus and Systems, Vol. PAS-90, No. 3, May-June 1971, pp. 1155-1165.

A3. E. Bridges et al.: “Measurement and Study of Radio Noise from Power lines in the Central Canada Region”, 1980, IEEE (CH-1538-8/80/0000-0021 \$00.75) pp. 21-25.

A4. Note by G.J. Nelson, “Proposed 132 kV Transmission Line near Culgoora” 28 may 1980, 7 pages.

A6. S. Pathak, G. Swarup A. Chatterjee and V. Kale, “Location of Radio Frequency Interference Using the GMRT”, paper presented at the General assembly of the International Radio Scientific Union, held at New Delhi, November 2005.

List of Figures and Captions

Figure Captions: Fig. Nos are in serial order for each Section

Section 1. Fig. S1-1: Layout of High Tension (H.T.) Power Lines supplying Power to the GMRT.

Section 2: Fig. S2-1: Gap discharge noise sources commonly found on power lines.

Section 2: Fig. S2-2: Radio noise field strength, peak detector, measured 9 ft. above the surface and 90 ft laterally from a pole on a 46-kV power line. Four gap-discharge noise sources on pole. (after Pakala et al., 1967)

Section 2: Fig. S2-3: Radio noise field strength, peak detector, measured 9 ft. above the surface and 50 ft laterally from a pole on a 4.16-kV distribution line. Gap-discharge noise source on the line (after Pakala et al., 1967)

Section 2: Fig. S2-4: A schematic three-phase A.C. 11 kV HT supply. RFI due to gap discharge may occur, when voltage rises to more than about 50% or 60% of 11 kV or there about on any of the three phase lines.

Section 3: Fig. S3-1: plots peak-electric noise field strength as a function of frequency for the interval of 10 kHz to 150 MHz at a lateral position of 200 ft from a steel tower supporting a single three-phase 244 kV AC transmission line.

Section 3: Fig. S3-2: Frequency spectra for conductor corona (fair weather) 200 ft. from outside phase of 244, 345, 525 and 735 kV AC lines (Pakala & Charter 1971)

Section 3: Fig. S3-3: Noise factor F_a versus frequency for various classes of line voltage ($P = F_a k \times 290 \times B = F_a \times 1.4 \times 10^{-23} \times 290 \times 106 = F_a \times -144 \text{ dBW/m}^2 / \text{Hz}$)

Section 3: Fig. S3-4: Flux Density ($\text{dBW m}^{-2} \text{Hz}^{-1}$); Approximate flux density of corona radiation at a distance of 200 ft from conductor at sea level (Thompson 1984; based on Charter's report 1984).

Section 3: Fig. 3-5: Electric Field ($\text{dB } \mu\text{V/m/120 kHz}$, quasi-peak) for a 362 KV line at 7000ft (Thompson 1984; based on Charter's report 1984)

Section 3: Fig. 3-6: Calculated relative lateral attenuation relative to 200 ft in dB, 25 to 10,000 MHz (Pakala & Chartier 1971). (Conductor Ht = 90 ft; receiving antenna Ht 10 ft).

Section 3: Fig. 3.7: Lateral attenuation (quasi-peak in dB) versus distance (ft) from centre phase at 30 MHz.

.Section 5: Fig. 5-1: Plot showing RFI at the GMRT antenna C2 due to 11 kV power lines across span of 50 MHz. The 150 MHz feed was pointed towards horizon and measurements were made using HP 8590L spectrum analyzer, with span 50 MHz, sweep time 40 ms, resolution bandwidth (RBW) as indicated below the plot and time constant inverse of VBW. (1998 April 29). Pulsed RFI by power-line is seen in the middle panel every 10 ms and gets averaged for 100 scans.

Section 5: Fig. 5-2: same as Fig. 5-1 but at 235 MHz in zero span mode, which acts as a total power receiver at 235 MHz, sweep 333 ms for the top and middle panel and 20 ms for the lower panel.

Section 5: Fig. 5-3: same as Fig. 5-1 and 5-2 but the 325 MHz primary feed of the C* antenna pointed to wards south with antenna in zenith position.

16-19: Section 5: Fig. 5-4, 5-5, 5-6, 5-7. Digital oscilloscope outputs at the base-band output of C02 antenna of GMRT showing sharp pulses due to 11kV pulsed RFI (measured by Swarup in 1998). Measurements were made with time constant of a circuit prior to the Digital Oscilloscope of 50 μ s, 500 ns, 1ms, 2.5 ms, 5ms and 250 ms. It is seen that pulse have a rise time of less than 500 ns but most of the power line RFI lies in $< \sim 0.5$ ms.

20:Section 5; Fig. 5-8, Power Spectrum of the pulsar receiver output for C2 antenna showing peaks at 50 Hz and odd multiples (Y Gupta 1995).

21-24: Section 6: Fig. S-1, S-2, S-3, and S-4: Measurements of powerline RFI at 150 MHz for 9 antennas (C0, C3, C8, C13, W2, W6, S1, S4, E2, and E5) made by Swarup and Raybole on 09-04-08 at the output of the optical fibre in the receiver room using a spectrum analyzer. Antennas were tracking 3C 48 around 5 PM. The 610 MHz feed was pointed towards the dish and hence the 150 MHz feed was towards the horizon. Span zero, sweep 21ms, RBW 300 kHz, VBW 300 kHz and line trigger. It is seen that pulsed RFI occurs mostly at every 10 ms. I have indicated in the margin as to which 11 kV phases give rise to the RFI. Very severe RFI is seen for the E2 antenna.

25-26: Section 6: Fig. S-5, S-6: Measurements of power line RFI at 239 MHz by Ajit Kumar and colleagues in 2003 at the base of GMRT antennas.

27: Section 12: Fig. 12-1 and 12-2: Schematic of a proposed clipping circuit for suppression of pulsed RFI at the base of each antenna.

Caption of Table I

Table I; measured values of Electrical strength of Radio Noise from HT Power-line and derived values of Flux Density, S (dB W m² Hz⁻¹) at 150 MHz

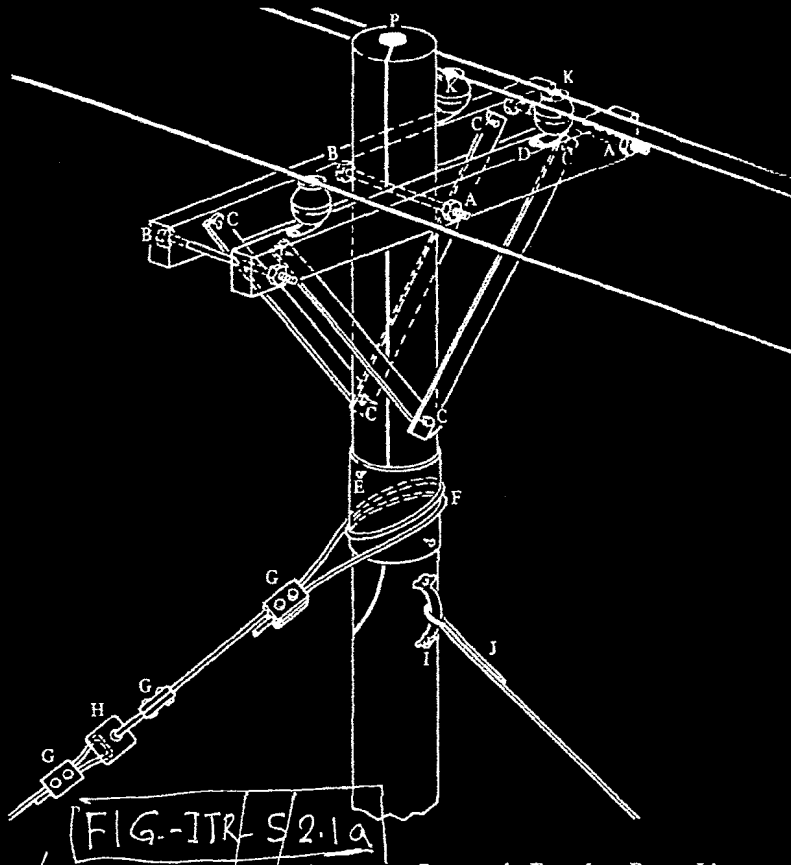


Fig. 3-1. Gap-discharge noise sources Commonly Found on Power Lines:

- | | |
|---|--------------------------------|
| A Retaining nut on crossarm | G Guy-wire shackle |
| B Retaining bolthead on crossarm | H Guy-wire insulator |
| C Crossarm brace bolthead and overlap joint | I Clete bolthead |
| D Insulator mounting post | J Guy-wire weld joint |
| E Metal-sleeve mounting bolthead | K Insulator to conductor joint |
| F Guy wire to metal-sleeve contact point | P Pole cap and grounding wire |

86 MAN-MADE RADIO NOISE

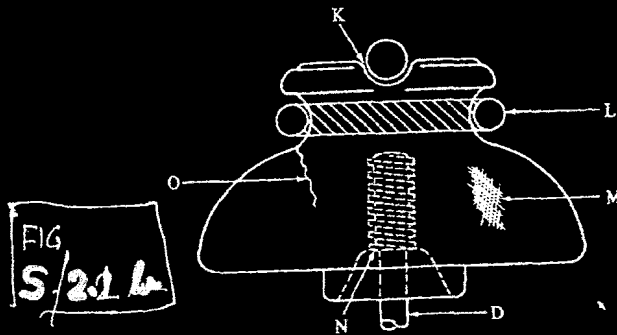


Fig. 3-2. Gap-discharge noise sources Commonly Found on Power-Line Insulators:

- | | |
|--------------------------------|---------------------------------|
| D Insulator mounting post | M Insulator contamination |
| K Insulator to conductor joint | N Insulator-mounting bolt joint |
| L Tie-wire contact joint | O Insulator fracture |

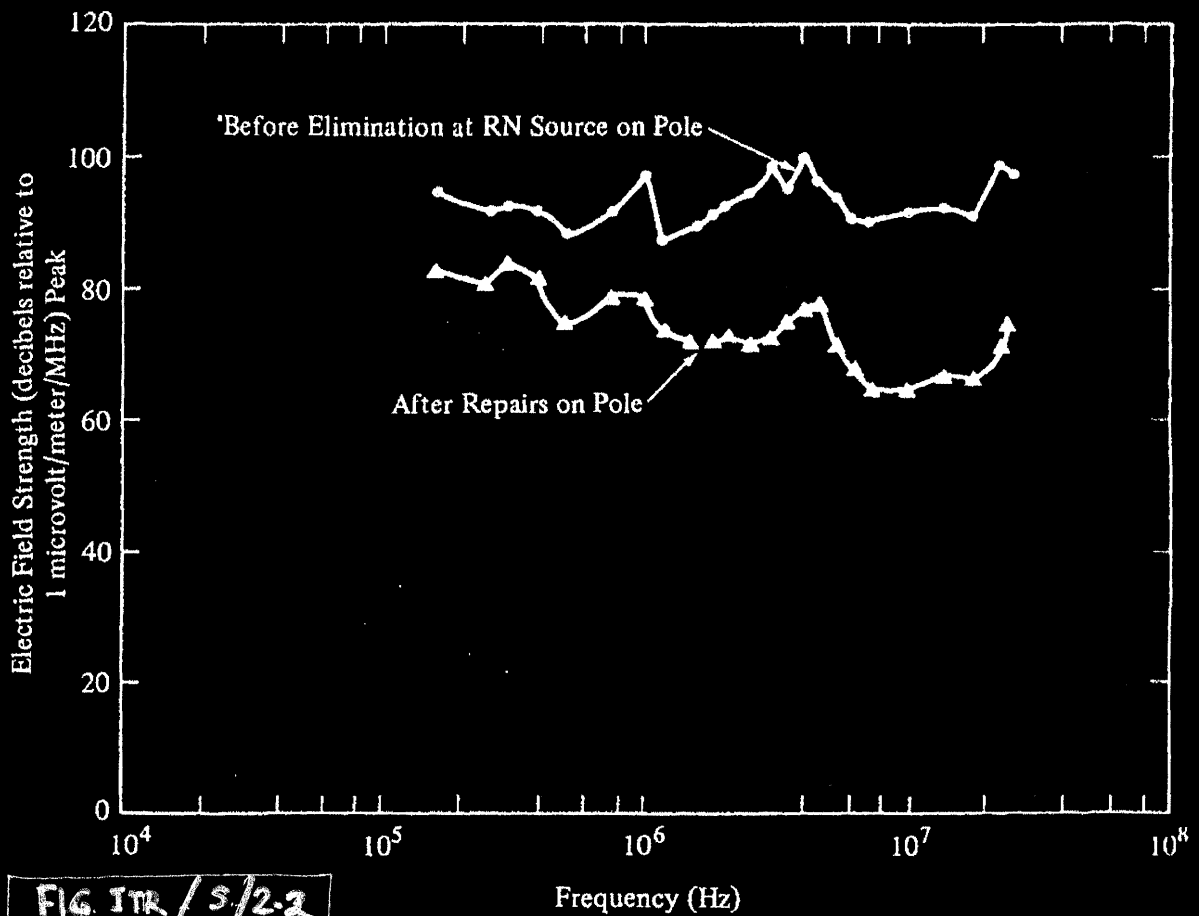


FIG. ITR / 5/2-2

Fig. 3-5. Radio-noise field strength, peak detector, measured 9 ft above the surface and 90 ft laterally from a pole on a 46-KV power line. Four gap-discharge noise sources on pole. (After Pakala et al., 1967)

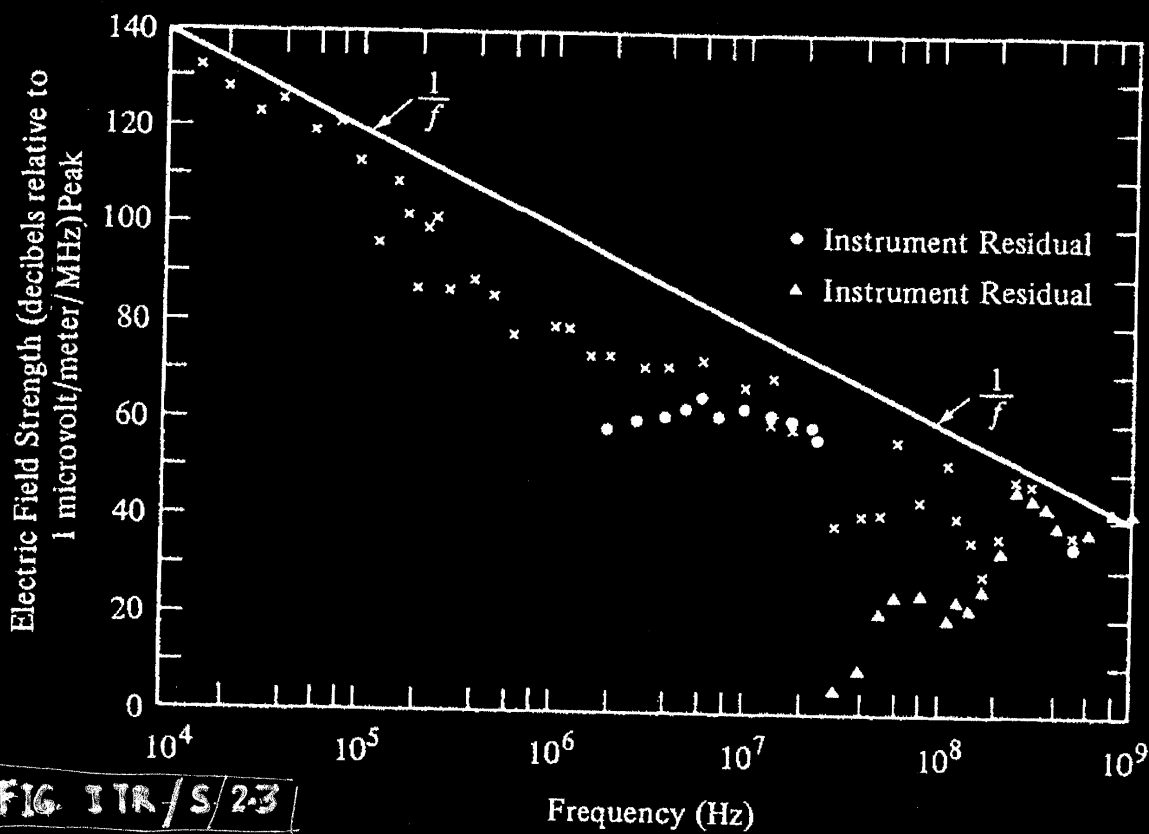
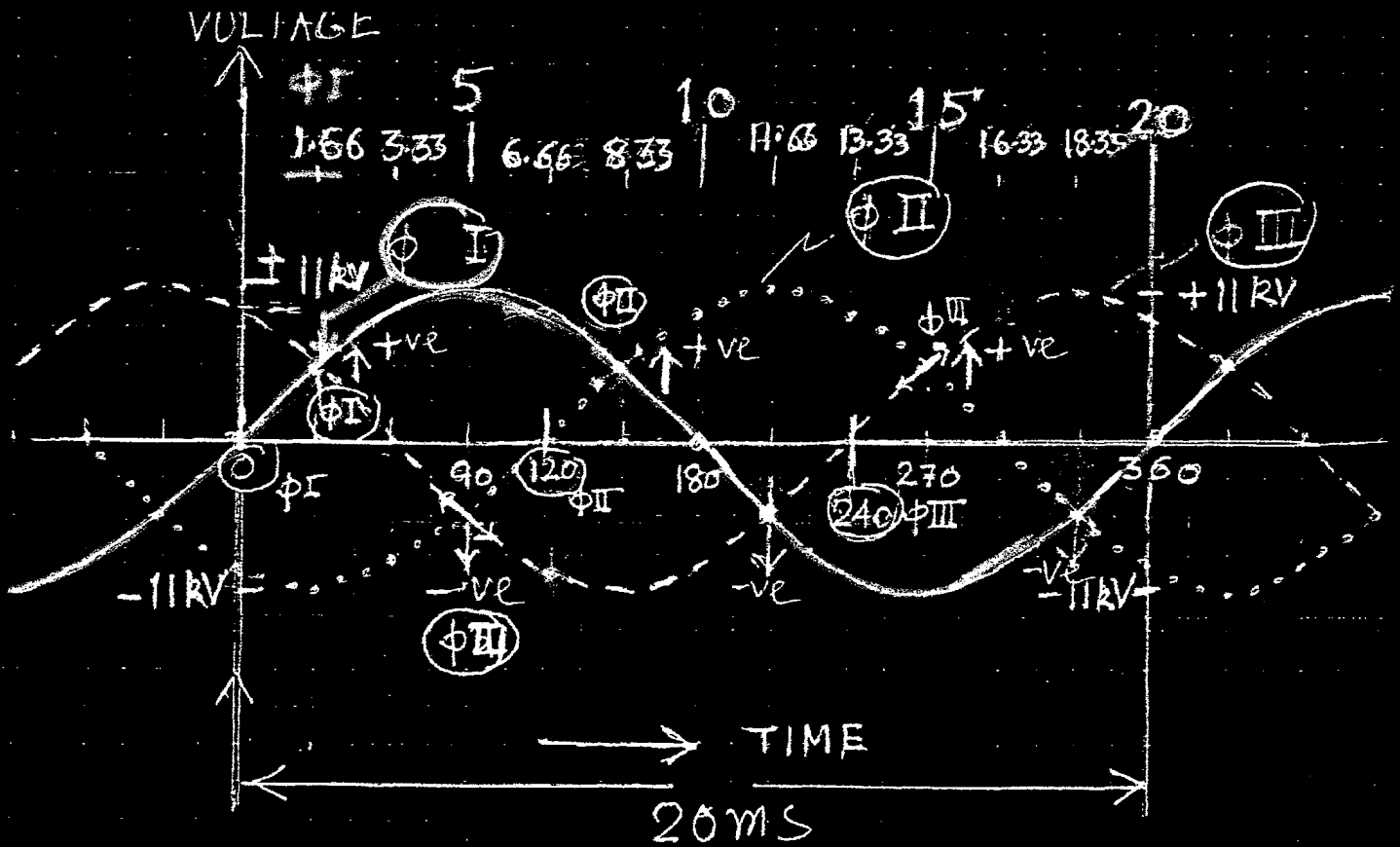


FIG ITR/S/23

Fig. 3-4) Radio-noise field strength, peak detector, measured 9 ft above the surface and 50 ft laterally from a 4.16-KV distribution line. Gap-discharge noise source on the line. (After Pakala et al., 1967)



$\Phi I \sim 1.5 - 3.3 \text{ ms}$	$\sim 11.5 - 13.3 \text{ ms}$
$\Phi II \sim 8.3 - 10 \text{ ms}$	$\sim 18.3 - 20 \text{ ms}$
$\Phi III \sim 5 - 6.6 \text{ ms}$	$15 - 16.6 \text{ ms}$

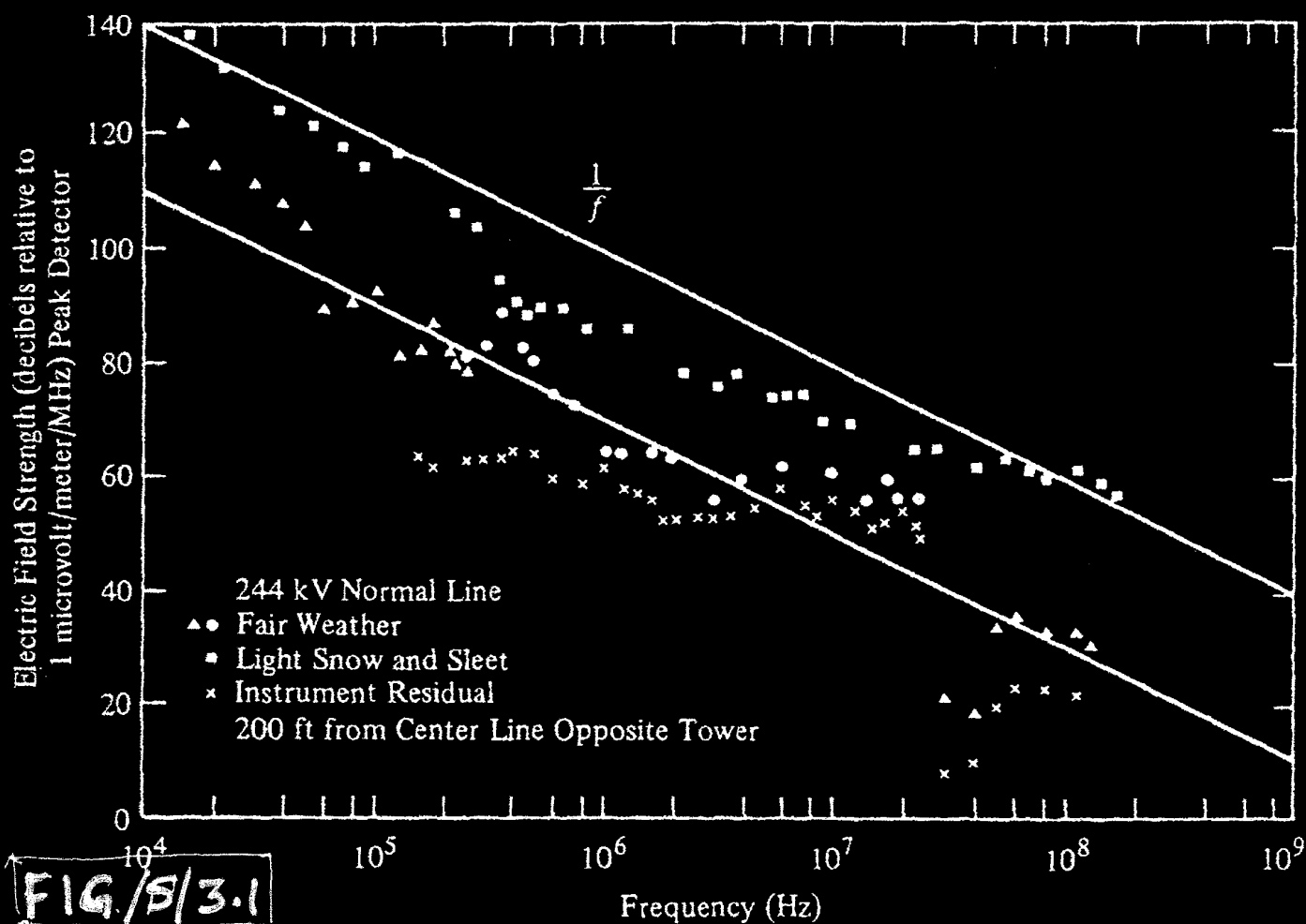
PERIODS WHEN GAP DISCHARGE MAY OCCUR

5/24

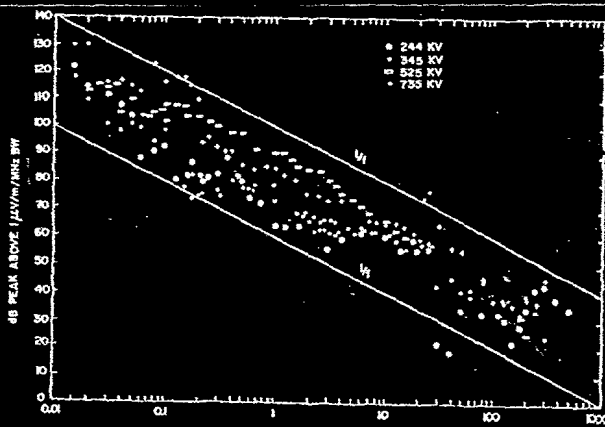
FIG. 2.4:

A schematic showing three-phase A.C. 11 kV HT supply. RFI due to gap discharge may occur, when Voltage rises to more than about 50% or 60% of 11 kV or thereabout on any of the three phase lines. It is noted from Fig. 7(a) 7(c) that pulsed RFI seems to occur on several occasions only every 10 ms, which indicates that only one of the three phases of 11 kV line shows RFI on a given day and RFI occurs only when voltage rises to + 11 kV or -11 kV (further measurements are required). The particular phase can be identified by measuring the time difference between the line trigger phase of the spectrum analyzer and the occurrence of pulsed RFI near the measured antenna of GMRT. In case of defective insulators or poor connections or poor grounding, it may be possible to identify the defective line by making RFI zero span ^{the measurements} using spectrum analyzer with trigger using power line voltage (not UPS) & identifying the phase.

Figure 3-16 plots peak-electric-noise field strength as a function of frequency for the interval of 10 kHz to 150 MHz obtained at a lateral offset position of 200 ft from a steel tower supporting a single three-phase 244-KV AC transmission line.⁸ The line was configured with horizontal conductors containing one cable per conductor; each cable was 1.246 in. in diameter. Line spacings of 28 ft and an elevation of



(SKOMEL) Fig. 3-16.) Peak electric noise field strength spectra for a 244-KV AC transmission line with corona noise sources. Measuring location: 200 ft laterally from a steel tower. (After Pakala et al., 1967)



→ dB(peak) $\mu\text{V}/\text{m}^2/\text{MHz}$

FIG/s/3-2 → f (MHz)

Fig. 10. Frequency Spectra for Conductor Corona (Fair Weather) at 200 Feet from Outside Phase of 244, 345, 525, and 735-kV ac Line
 PAKALA & CHARTIER FIG. 10

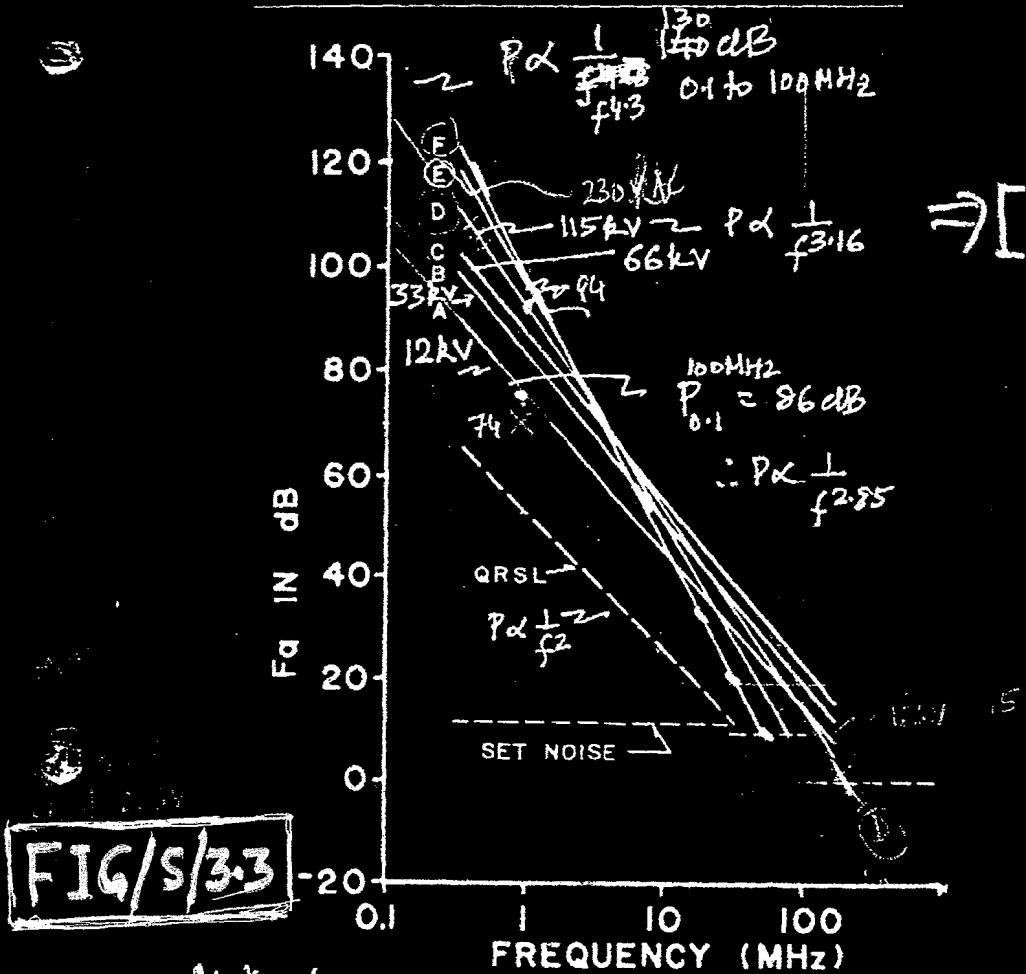
The linear model equation for F_a has the form

$$F_a = \alpha \log f + \beta$$

where f is the frequency in MHz, α is the slope in dB per frequency decade and β is the intercept (the value of F_a at 1 MHz). Fig. 1 shows that β for each voltage class increases with voltage from a value of 74 dB for the 12 kV class to 94 dB for the 230 kV class for ac lines and to 97 dB for the 450 kV dc line.

LEGEND	LINE VOLTAGE (kV)	NUMBER OF SITES	NUMBER OF SAMPLES
A	12	1	104
B	33	1	96
C	66	1	93
D	115	5	480
E	230	4	329
F	450 dc	1	99

All measurements 50 ft from line centre



Notes by CS30/6/08

RMS values across 50 ohm

Fig. 1 F_a versus frequency for various classes of line voltage.

$$\therefore P = 1.4 \times 10^{-23} \times 290 \times 10^6 \cdot F_a = F_a \times -144 \text{ dBW/m}^2/\text{Hz}$$

The slope α decreases with increasing class voltage and has values of -30 dB/decade for the 12 kV class, -45 dB/decade for the 230 kV class and -63 dB/decade for the 450 kV dc line. It is interesting to note that the models for the three highest

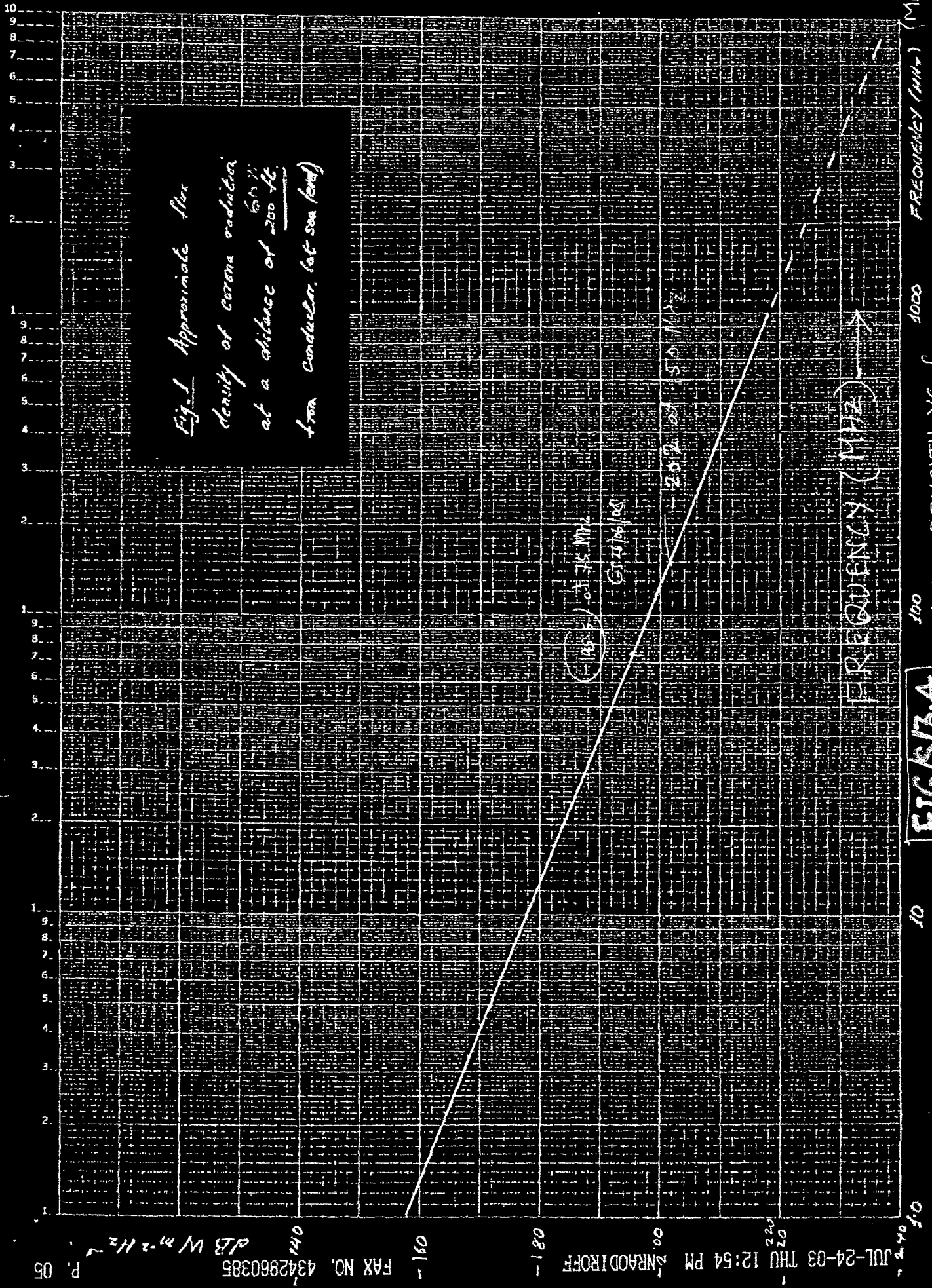
1 MHz

$$F_a = F_a \cdot \ln \frac{1}{\Delta f} \approx 1 \text{ MHz}$$

$$F_a = F_a \cdot 1.4 \times 10^{-23} \times 290 \times 10^6$$

$$P(100 \text{ MHz}) = 10^{-16} \text{ W/m}^2/\text{MHz} \times 10^2$$

at RMS



FIG/S/3.4

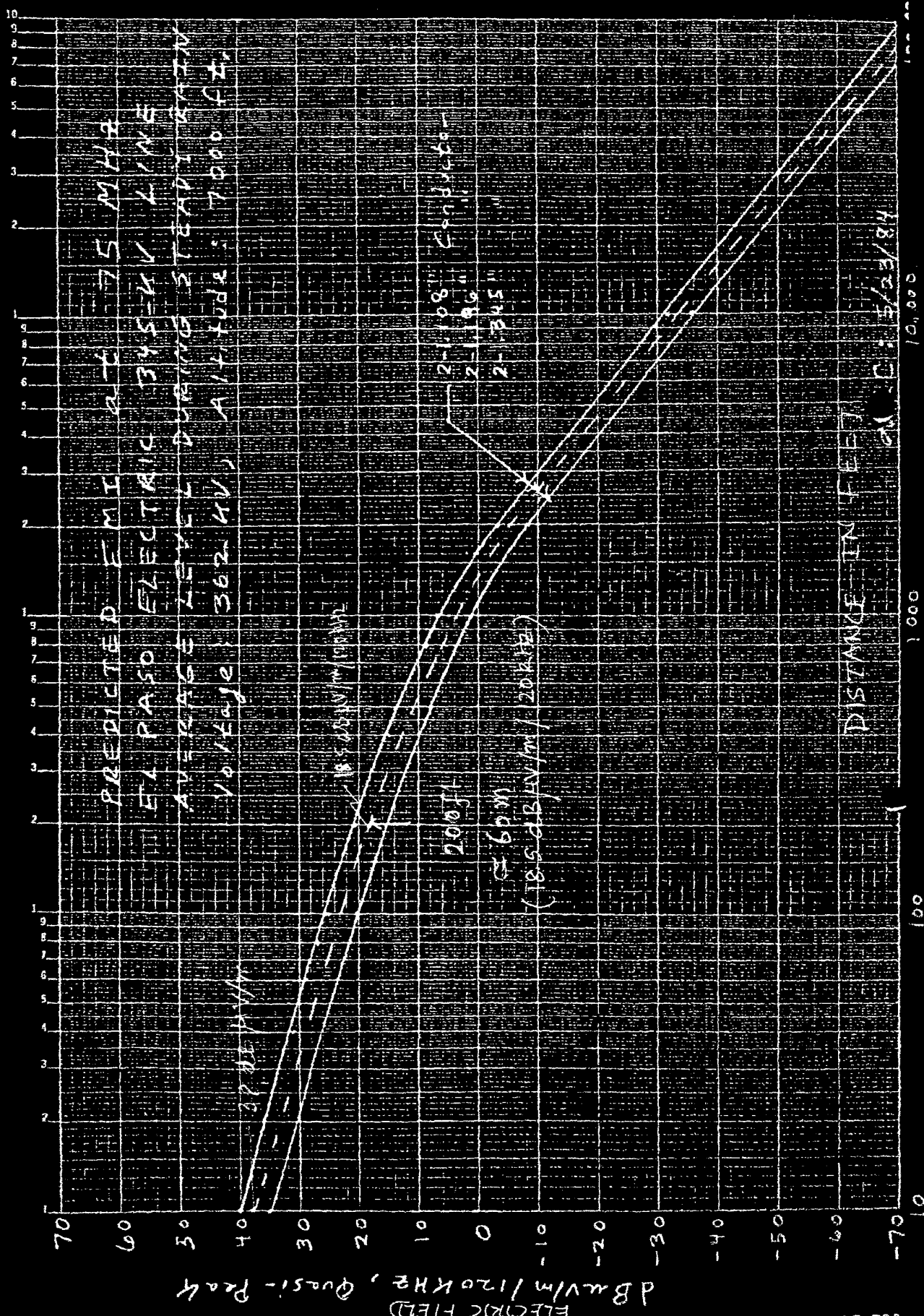
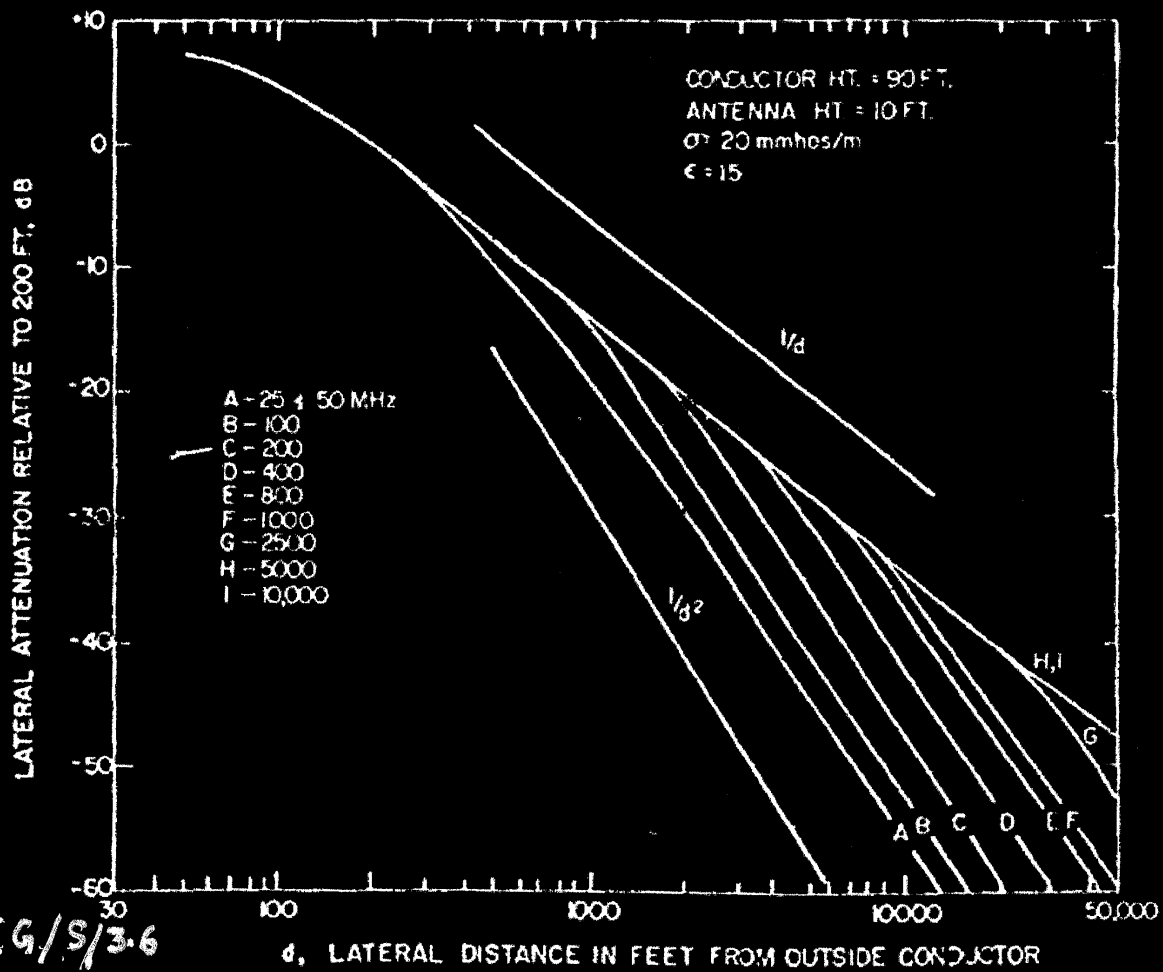


FIG 3.5



FIG/S/3-6

d, LATERAL DISTANCE IN FEET FROM OUTSIDE CONDUCTOR

PAKALA + CHARTIER

Fig. 14. Calculated Relative Lateral Attenuation, 25 to 10,000 MHz,

5-

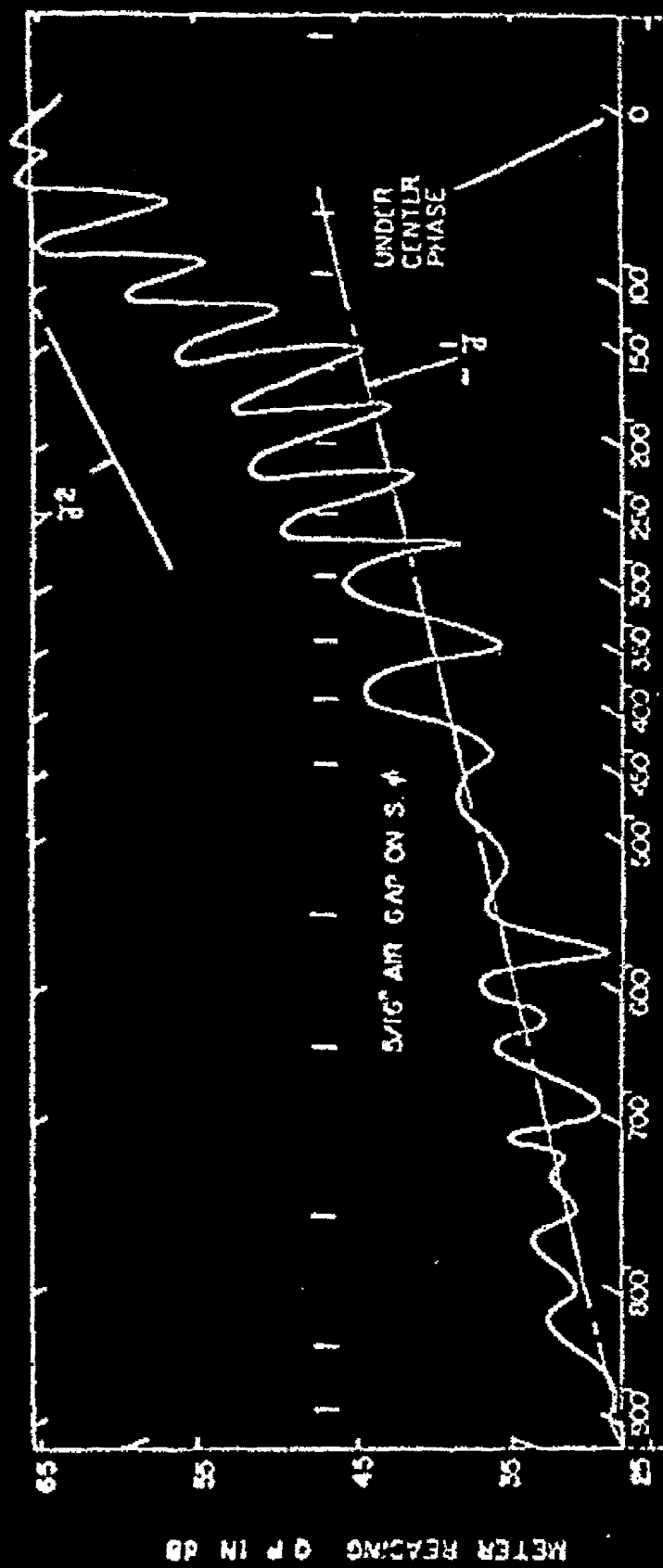


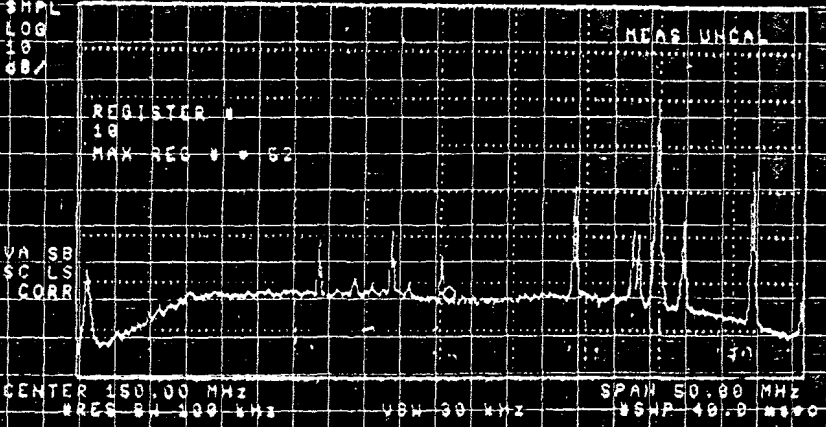
FIG. 5/3.7

Patola + Chorghar 1973

Fig. 15. *Lateral Attenuation with 5/16-Inch Gap Made with Chart Recorder at 30 MHz. Gap on Outside Phase.*

17:31:23 APR 29, 1998
 10:49:52 APR 29, 1998
 REF -5.0 dBm AT 10 dB
 MKR 150.63 MHz
 -69.18 dBm

(10) 150 MHz



2-N
 RF=0W
 RBW=100kHz
 Average
 100 SCANS
 Average 100
 SCANS

CENTER 150.00 MHz
 RES BW 100 kHz
 SPAN 50.00 MHz
 VBW 30 kHz
 VBWP 40.0 MHz

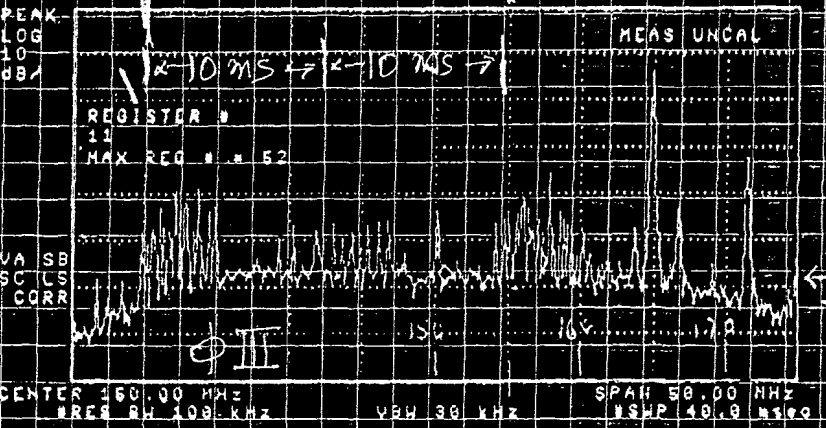
125

175

← 20 ms →

17:31:49 APR 29, 1998
 10:50:17 APR 29, 1998
 REF -5.0 dBm AT 10 dB
 MKR 150.63 MHz
 -69.72 dBm

(11)



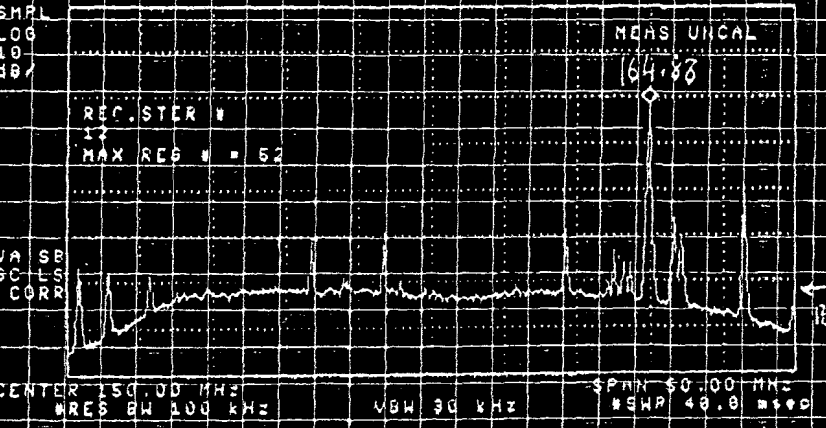
MSEB POWER
 ON
 Do
 SINGLE SCAN
 Single
 RBW=100kHz

CENTER 150.00 MHz
 RES BW 100 kHz
 SPAN 50.00 MHz
 VBW 30 kHz
 VBWP 40.0 MHz

BW=100 kHz

17:32:13 APR 29, 1998
 10:55:13 APR 29, 1998
 REF -5.0 dBm AT 10 dB
 MKR 164.88 MHz
 -26.62 dBm

(12)



DO
 AVERAGE
 100 SCANS
 BL = -68 dBm
 RF=0W
 MSEB

CENTER 150.00 MHz
 RES BW 100 kHz
 SPAN 50.00 MHz
 VBW 30 kHz
 VBWP 40.0 MHz

5.1 1998 April 29

FIG. 5.1 : Plot showing RFI at GMRT antennas due to 11 kV power lines. 150 MHz antenna feed was pointed towards horizon and measurements made using HP 8590L Spectrum Analyzer in Zero Span Mode, which acts as a total power receiver with Resolution Bandwidth (RBW) as indicated below the plot and time constant inverse of VBW. Plot shows RFI at 150 MHz and 164.88 MHz.

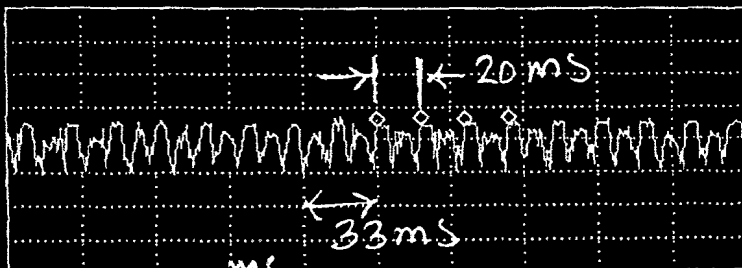
2nd JAN 98

235 MHz feed to WEST

17:26:33 02 JAN 1998
 16:05:00 02 JAN 1998
 REF -10.0 dBm #AT 0 dB

MKR 226.67 msec
 -46.15 dBm

PEAK
 LOG
 10
 dB/



Time Domain Plot.
 at 10µs integ. times

ZERO SPAN

Marker	Trace Type	ms	Freq / Time	Amplitude
1:	(A)	Time 20.0	166.67 MS	-46.79 dBm
2:	(A)	Time 20.0	186.67 MS	-45.76 dBm
3:	(A)	Time 20.0	206.67 MS	-46.31 dBm
4:	(A)	Time 20.0	226.67 MS	-46.15 dBm

CENTER 235.000 MHz SPAN 0 Hz
 #RES BW 300 kHz VBW 100 kHz SWP 333 msec

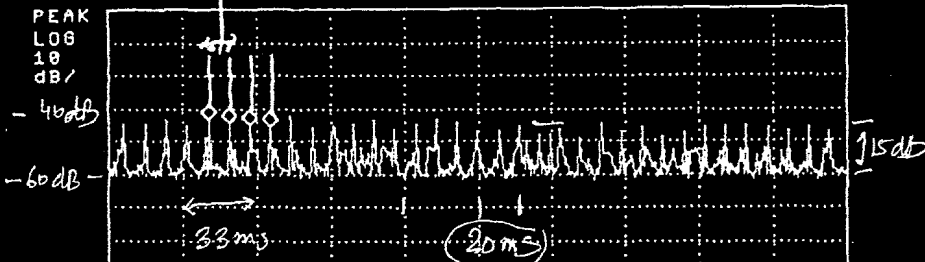
Sweep 333 msec

9.167 ms

17:29:12 02 JAN 1998
 16:05:49 02 JAN 1998
 REF -10.0 dBm #AT 0 dB

MKR 72.500 msec
 -46.20 dBm

PEAK
 LOG
 10
 dB/



(" ")

Marker	Trace Type	ms	Freq / Time	Amplitude
1:	(A)	Time 9.167	45.000 MS	-43.79 dBm
2:	(A)	Time 9.167	54.167 MS	-45.10 dBm
3:	(A)	Time 9.167	63.333 MS	-45.35 dBm
4:	(A)	Time 9.167	72.500 MS	-46.20 dBm

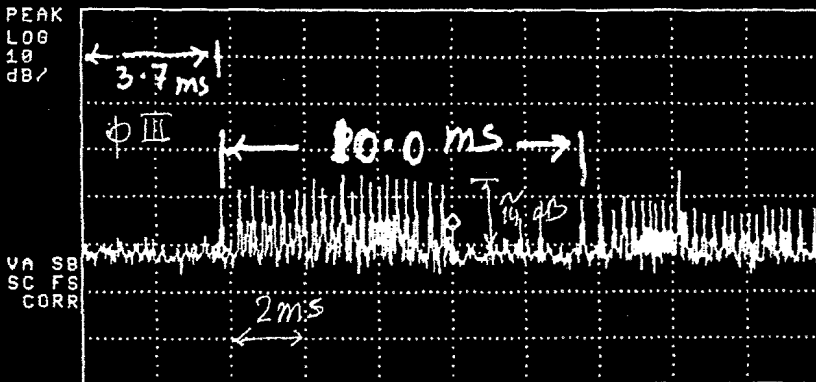
CENTER 235.000 MHz SPAN 0 Hz
 #RES BW 300 kHz VBW 100 kHz SWP 333 msec

$$\frac{1s}{9.167ms^2} = \frac{10^9}{84} = 54.5 Hz = \text{freq of MSEC on that day!}$$

17:29:52 02 JAN 1998
 16:07:59 02 JAN 1998
 REF -10.0 dBm #AT 0 dB

MKR 235.000 MHz
 -57.23 dBm

PEAK
 LOG
 10
 dB/



Freq. Domain Plot

→ 3MHz BW around 235 MHz.

RFI Burst seen with 10µs integ. time.

CENTER 235.000 MHz SPAN 3.000 MHz
 #RES BW 300 kHz VBW 100 kHz SWP 20.0 msec

FIG 5-2

BW 300 kHz

SWEEP TIME 20 ms

MS

FIG. 5-2 Same as Fig. 5-1 but at 235 MHz

5.

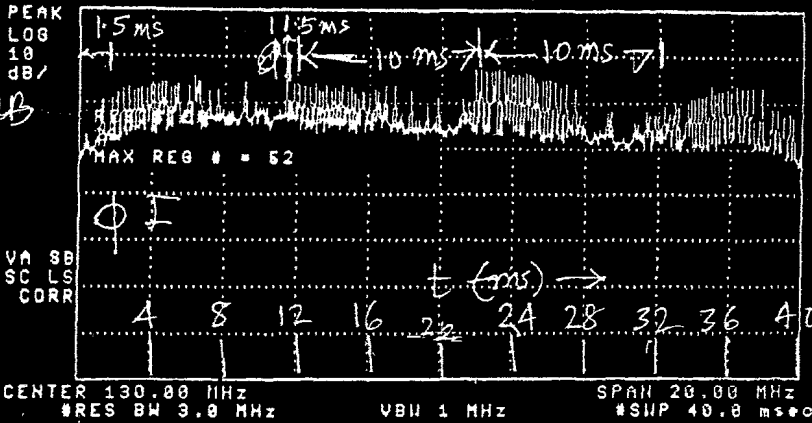
98 Apr 29 ✓

325 MHz C8 - S

(26)

GJ

14:18:42 APR 29, 1998
19:15:51 APR 28, 1998
REF .0 dBm AT 10 dB



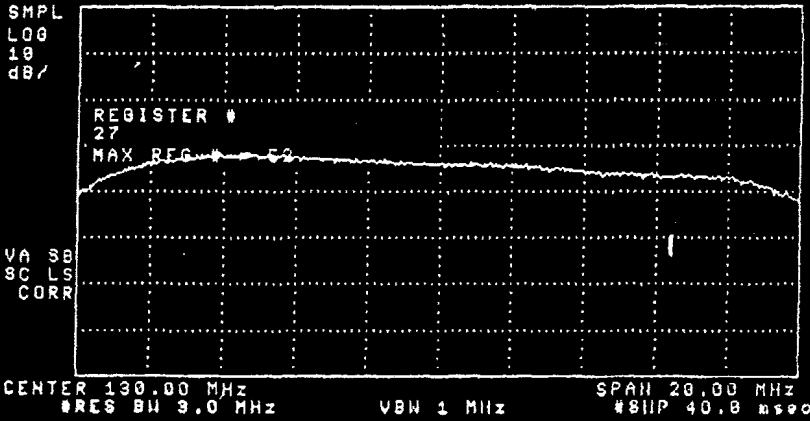
~10dB

Φ I

325 MHz C8 - S Averaged 100 SCANS

(27)

14:19:20 APR 29, 1998
19:16:49 APR 28, 1998
REF .0 dBm AT 10 dB



C8 - S 325

(29)

14:19:53 APR 29, 1998
19:18:08 APR 28, 1998
REF .0 dBm AT 10 dB

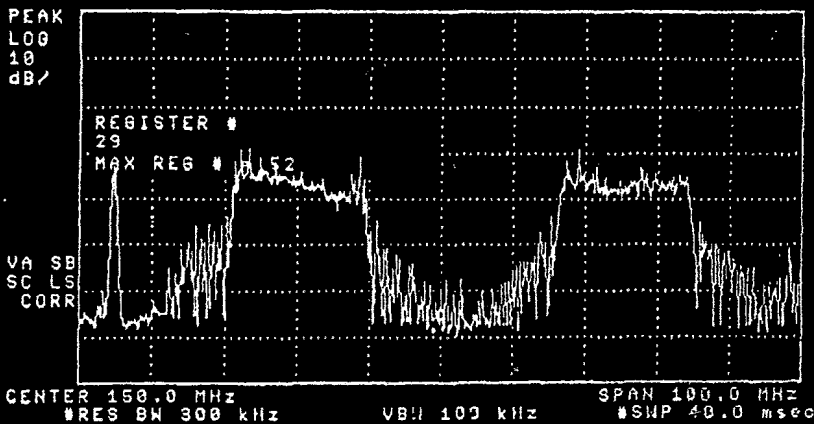


FIG. 7(2) Same as Fig. 7(2) but at 325 MHz.

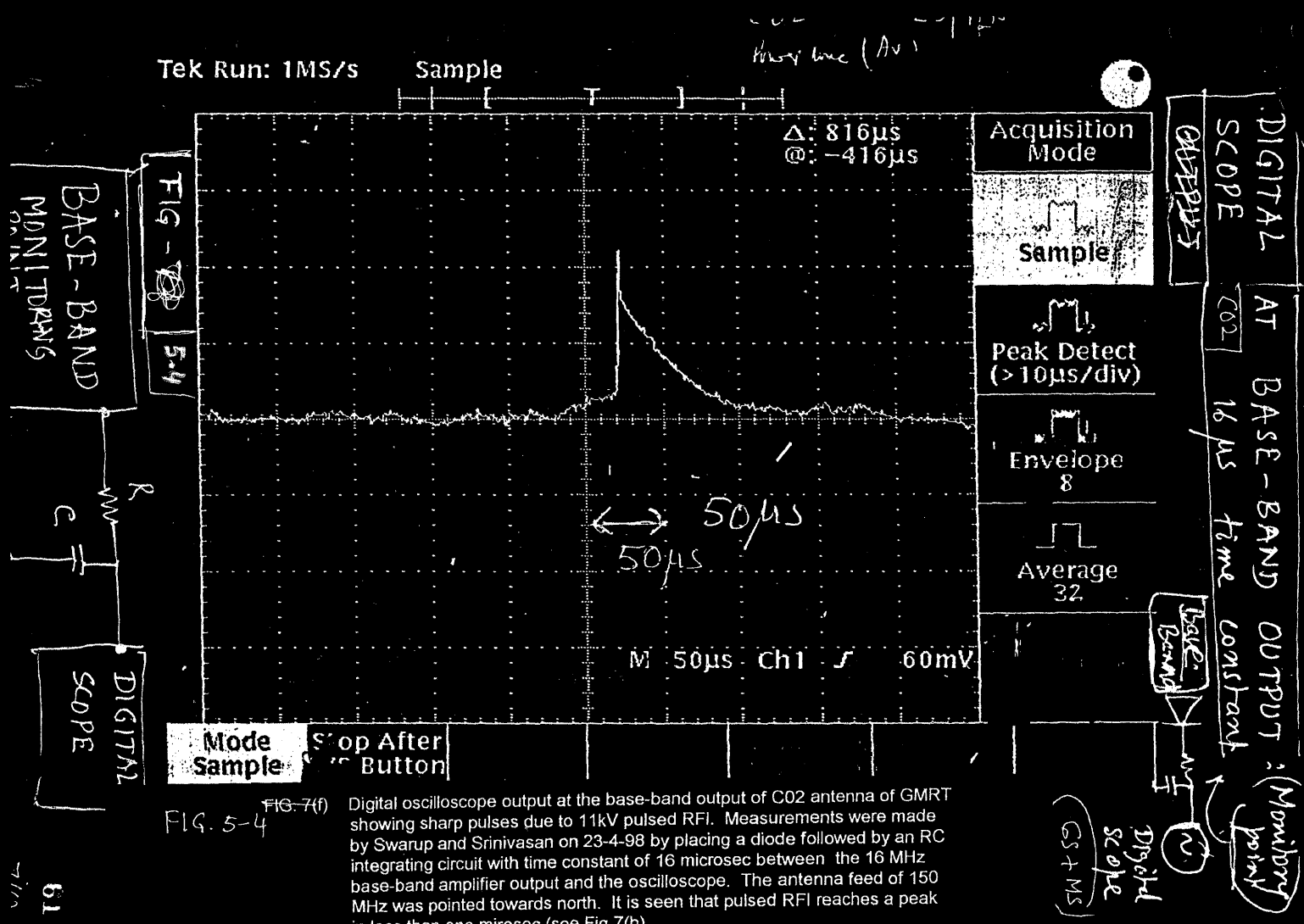


FIG. 5-4

FIG. 7(f) Digital oscilloscope output at the base-band output of C02 antenna of GMRT showing sharp pulses due to 11kV pulsed RFI. Measurements were made by Swarup and Srinivasan on 23-4-98 by placing a diode followed by an RC integrating circuit with time constant of 16 microsec between the 16 MHz base-band amplifier output and the oscilloscope. The antenna feed of 150 MHz was pointed towards north. It is seen that pulsed RFI reaches a peak in less than one microsec (see Fig 7(h)).

C-2 24104
4:05

GS+MS

C-2 24/4/98

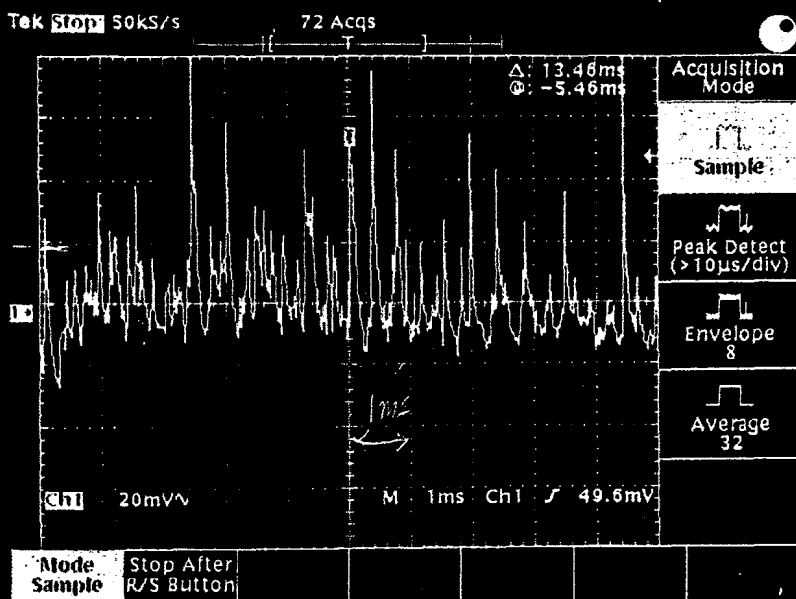


Fig. 4(PP)

C-2

4:08

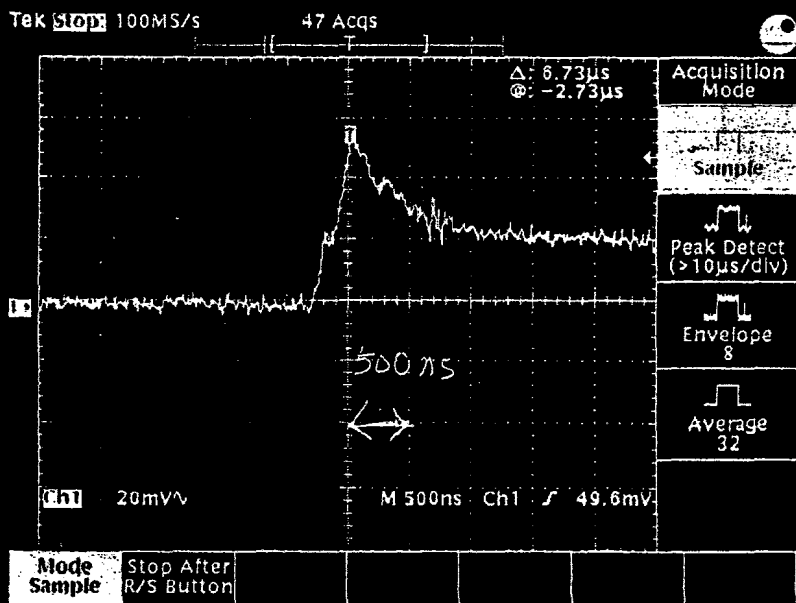


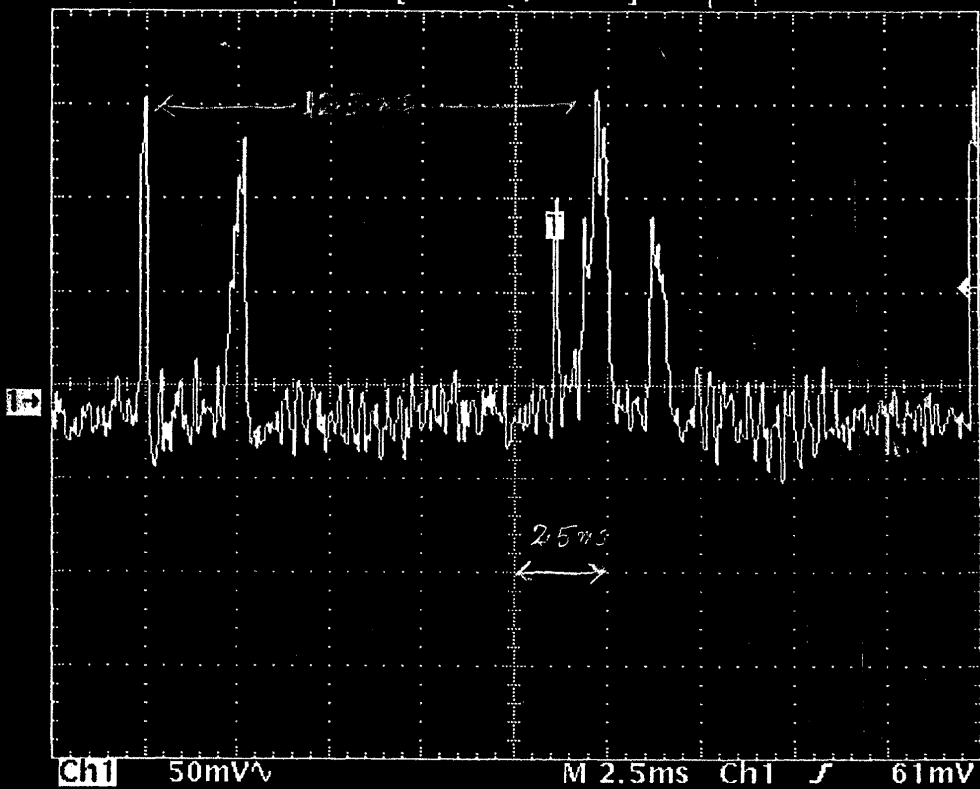
FIG. 5-5

5-4

FIG. 4(PP): Same as Fig. 7(PP) with 1 ms and 500 ns respectively.

Tek Stop 20kS/s

13 Acqs



Δ: 40.8ms
@: -20.8ms

Ch1 Period
2.591ms

Ch1 Period
2.591ms

ch1 50mV M 2.5ms Ch1 J 61mV

Fig. 7(5) 5-6

2.5ms

5-6
FIG. 7(1) Same as Fig. 7(1) with 2.5 ms

5-4

S-2

24/04/98

3:50

GS +

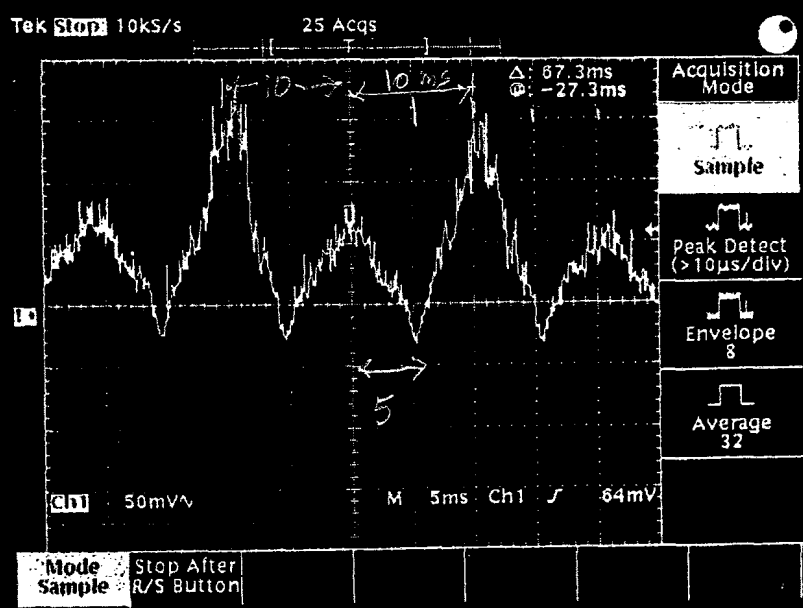


Fig. 7(j)

5ms

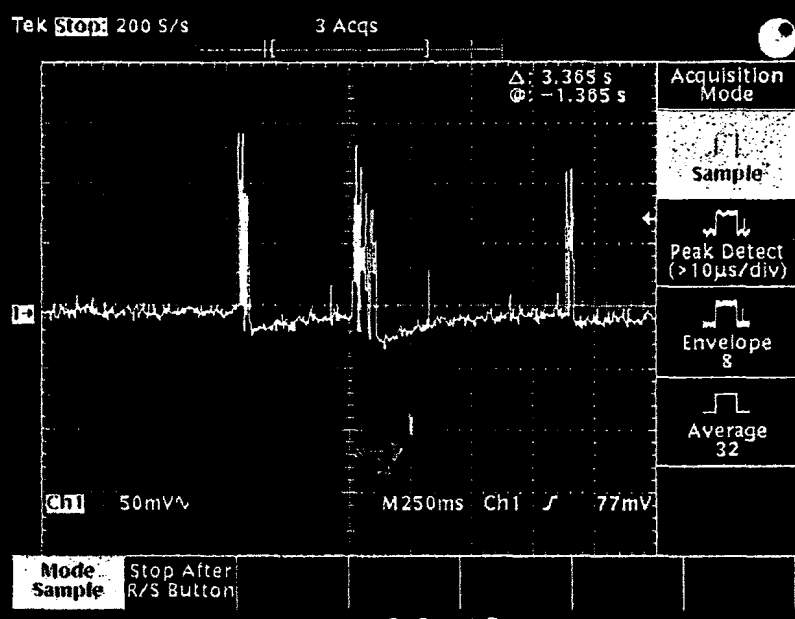


FIG. 7(j) and (k): Same as Fig. 7(i) with 250 ms.

5.7

250ms

5-1

Line freq. interference from GA
Amplitude spectrum of pulsar signal for DM = 0.0

29/3/95

14:07 hrs.

25 secs
of data

Yash Gupta

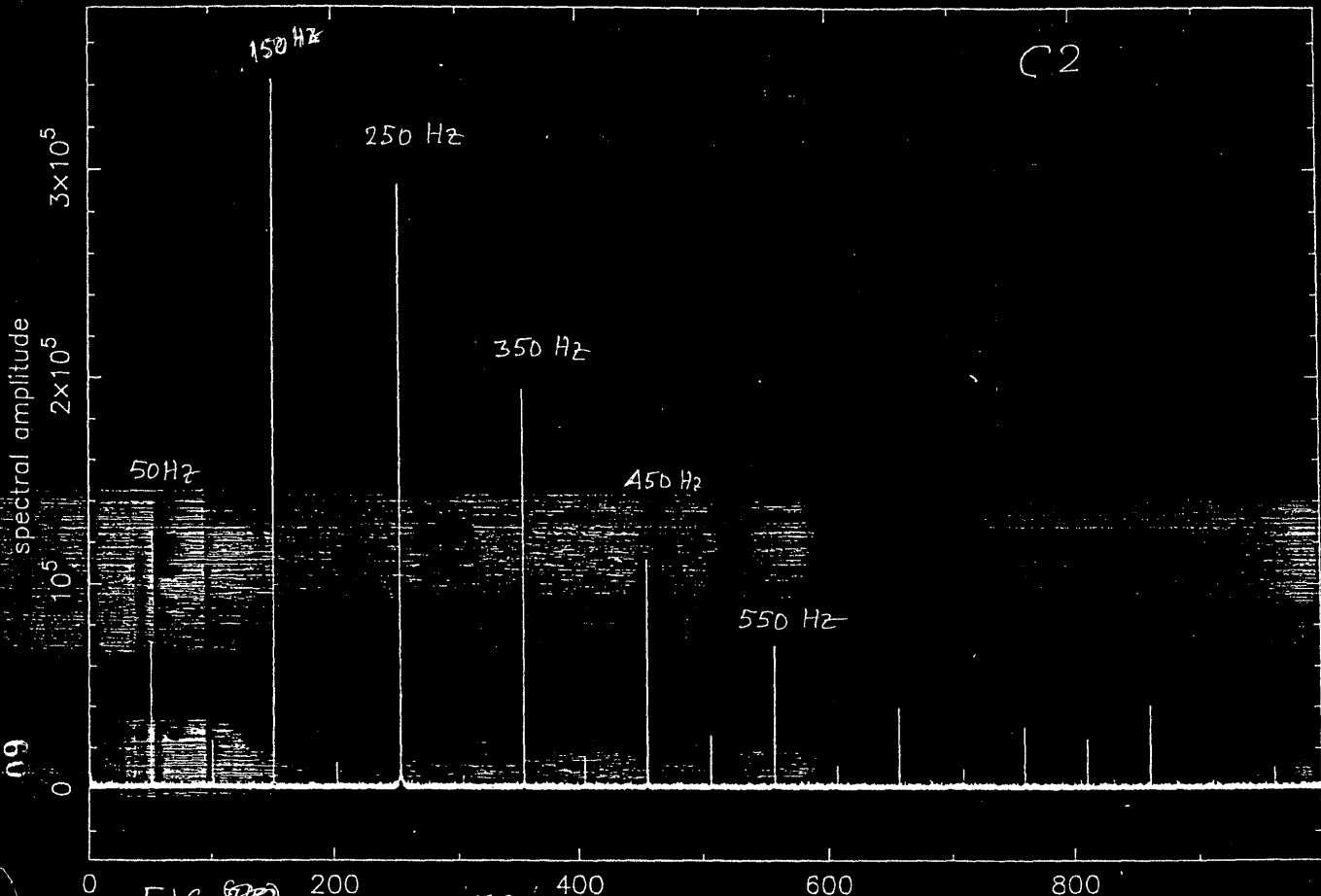


FIG. 7(a)
5-8

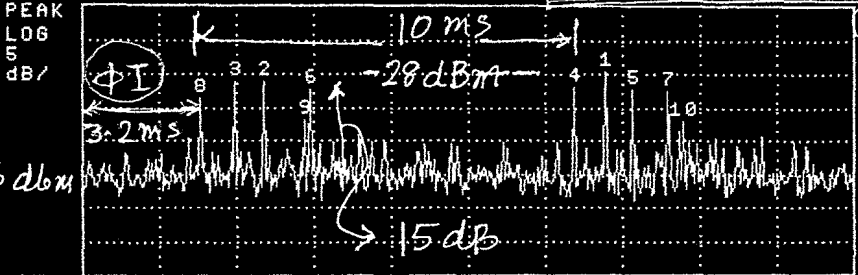
FIG. 7(a) Power Spectrum of the pulsar receiver output showing peaks at 50 Hz and odd multiples (power spectrum outputs are different on other days).

C2

09-04-08

09:33:29 09 APR 2008
16:54:49 08 APR 2008
REF -18.0 dBm #AT 0 dB

① C0 - 150 MHz - towards horizon



② Antennas tracking 3C48 ~ 5PM
610 MHz feed to focus

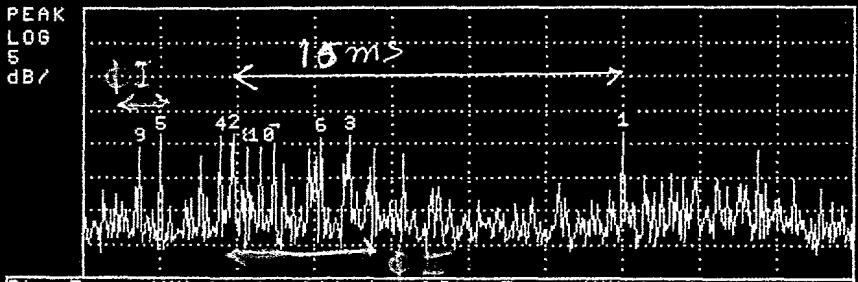
Pk	Freq (MHz)	Amplitude	Pk	Freq (MHz)	Amplitude
1	130.000	-27.73 dBm	6	130.000	-30.28 dBm
2	130.000	-29.05 dBm	7	130.000	-30.47 dBm
3	130.000	-29.10 dBm	8	130.000	-31.80 dBm
4	130.000	-30.05 dBm	9	130.000	-34.85 dBm
5	130.000	-30.21 dBm	10	130.000	-35.21 dBm

CENTER 130.000 MHz SPAN 0 Hz
#RES BW 300 kHz #VBW 300 kHz #SWP 21.0 msec

③ LINE TRIGGER

09:34:45 09 APR 2008
16:56:17 08 APR 2008
REF -18.0 dBm #AT 0 dB

C3 - 150 MHz



① I
~15dB

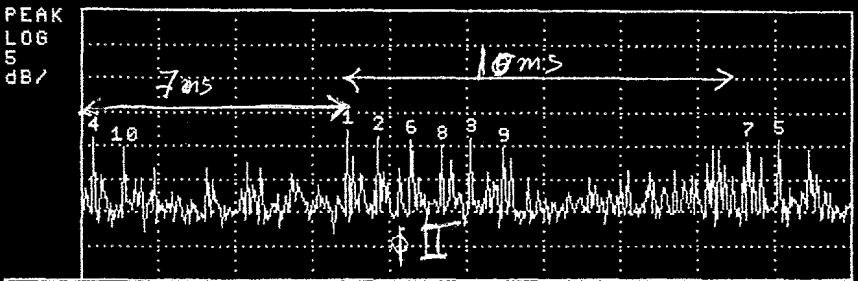
Pk	Freq (MHz)	Amplitude	Pk	Freq (MHz)	Amplitude
1	130.000	-35.32 dBm	6	130.000	-37.16 dBm
2	130.000	-36.52 dBm	7	130.000	-38.11 dBm
3	130.000	-36.89 dBm	8	130.000	-38.44 dBm
4	130.000	-36.94 dBm	9	130.000	-38.63 dBm
5	130.000	-36.99 dBm	10	130.000	-38.63 dBm

CENTER 130.000 MHz SPAN 0 Hz
#RES BW 300 kHz #VBW 300 kHz #SWP 21.0 msec

09-04-08

09:35:17 09 APR 2008
16:57:15 08 APR 2008
REF -31.0 dBm #AT 0 dB

C8 - 150 MHz



② II
~13dB

Pk	Freq (MHz)	Amplitude	Pk	Freq (MHz)	Amplitude
1	130.000	-48.79 dBm	6	130.000	-50.26 dBm
2	130.000	-49.51 dBm	7	130.000	-50.31 dBm
3	130.000	-49.72 dBm	8	130.000	-51.00 dBm
4	130.000	-49.94 dBm	9	130.000	-51.31 dBm
5	130.000	-50.03 dBm	10	130.000	-51.36 dBm

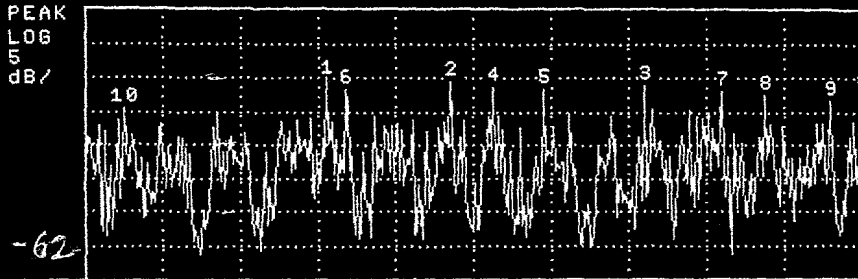
CENTER 130.000 MHz SPAN 0 Hz
#RES BW 300 kHz #VBW 300 kHz #SWP 21.0 msec

FIG/S/G-1

GS + PAR

09:36:20 09 APR 2008
 16:59:39 08 APR 2008
 REF -27.0 dBm #AT 0 dB

C13 - 150 MHz



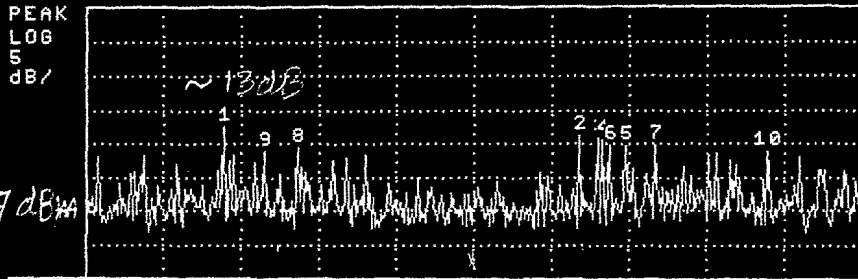
Pk	Freq (MHz)	Amplitude	Pk	Freq (MHz)	Amplitude
1	130.000	-37.25 dBm	6	130.000	-38.78 dBm
2	130.000	-37.63 dBm	7	130.000	-38.94 dBm
3	130.000	-38.27 dBm	8	130.000	-39.65 dBm
4	130.000	-38.43 dBm	9	130.000	-40.41 dBm
5	130.000	-38.66 dBm	10	130.000	-41.47 dBm

CENTER 130.000 MHz SPAN 0 Hz
 #RES BW 300 kHz #VBW 300 kHz #SWP 21.0 msec

④

09:36:53 09 APR 2008
 17:00:40 08 APR 2008
 REF -27.0 dBm #AT 0 dB

W2 - 150 MHz



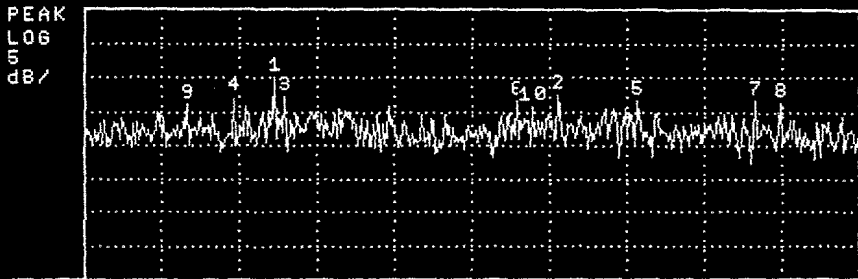
Pk	Freq (MHz)	Amplitude	Pk	Freq (MHz)	Amplitude
1	130.000	-44.38 dBm	6	130.000	-47.34 dBm
2	130.000	-45.80 dBm	7	130.000	-47.41 dBm
3	130.000	-46.05 dBm	8	130.000	-47.49 dBm
4	130.000	-46.37 dBm	9	130.000	-48.24 dBm
5	130.000	-47.27 dBm	10	130.000	-48.25 dBm

CENTER 130.000 MHz SPAN 0 Hz
 #RES BW 300 kHz #VBW 300 kHz #SWP 21.0 msec

⑤

09:37:30 09 APR 2008
 17:01:20 08 APR 2008
 REF -27.0 dBm #AT 0 dB

W6 - 150 MHz



Pk	Freq (MHz)	Amplitude	Pk	Freq (MHz)	Amplitude
1	130.000	-37.12 dBm	6	130.000	-40.42 dBm
2	130.000	-39.58 dBm	7	130.000	-40.55 dBm
3	130.000	-39.79 dBm	8	130.000	-40.84 dBm
4	130.000	-40.00 dBm	9	130.000	-41.13 dBm
5	130.000	-40.38 dBm	10	130.000	-41.25 dBm

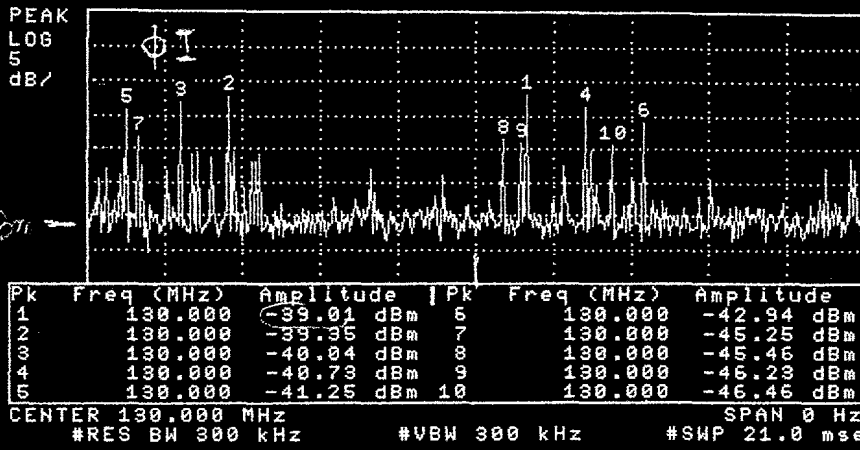
CENTER 130.000 MHz SPAN 0 Hz
 #RES BW 300 kHz #VBW 300 kHz #SWP 21.0 msec

⑥

Fig/S/6-2

09:42:43 09 APR 2008
 17:01:56 08 APR 2008
 REF -27.0 dBm #AT 0 dB

S1 - 150 MHz



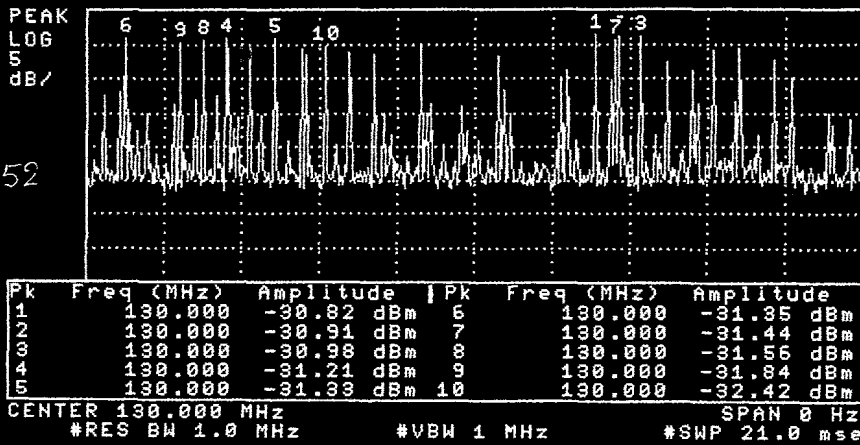
7

-60 dBm

~23 dB ϕI

09:43:42 09 APR 2008
 17:02:31 08 APR 2008
 REF -27.0 dBm #AT 0 dB

S1 - 150 MHz



8

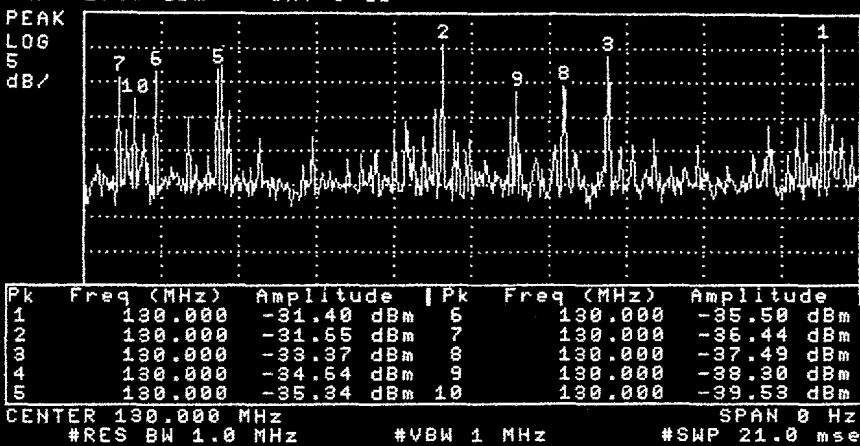
-52

All 3 phases?

~25 dB

09:44:30 09 APR 2008
 17:03:10 08 APR 2008
 REF -27.0 dBm #AT 0 dB

S4 - 150 MHz



9

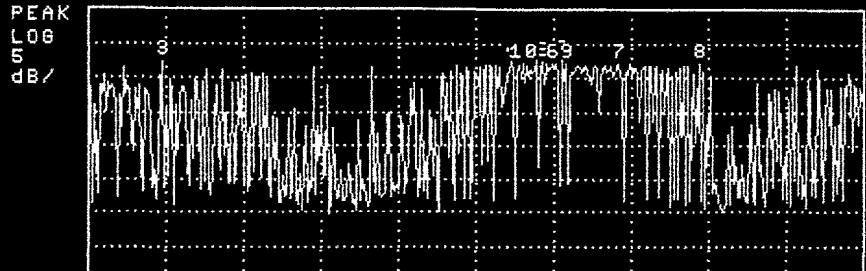
ϕI

~21 dB

Fig 5/6-3

09:46:20 09 APR 2008
 17:04:35 08 APR 2008
 REF -18.5 dBm #AT 0 dB

E2 - 150 MHz



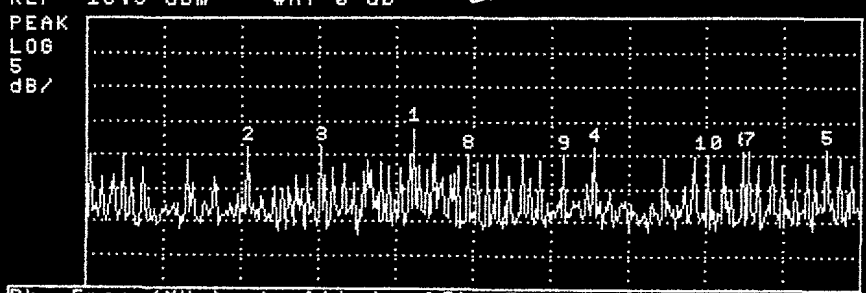
Pk	Freq (MHz)	Amplitude	Pk	Freq (MHz)	Amplitude
1	130.000	-25.94 dBm	6	130.000	-26.38 dBm
2	130.000	-26.01 dBm	7	130.000	-26.40 dBm
3	130.000	-26.27 dBm	8	130.000	-26.50 dBm
4	130.000	-26.31 dBm	9	130.000	-26.54 dBm
5	130.000	-26.34 dBm	10	130.000	-26.61 dBm

CENTER 130.000 MHz SPAN 0 Hz
 #RES BW 1.0 MHz #VBW 1 MHz #SWP 21.0 msec

(10)

09:47:04 09 APR 2008
 17:05:00 08 APR 2008
 REF -18.5 dBm #AT 0 dB

E5 - 150 MHz



Pk	Freq (MHz)	Amplitude	Pk	Freq (MHz)	Amplitude
1	130.000	-34.64 dBm	6	130.000	-37.82 dBm
2	130.000	-37.22 dBm	7	130.000	-38.06 dBm
3	130.000	-37.27 dBm	8	130.000	-38.46 dBm
4	130.000	-37.48 dBm	9	130.000	-38.46 dBm
5	130.000	-37.64 dBm	10	130.000	-38.46 dBm

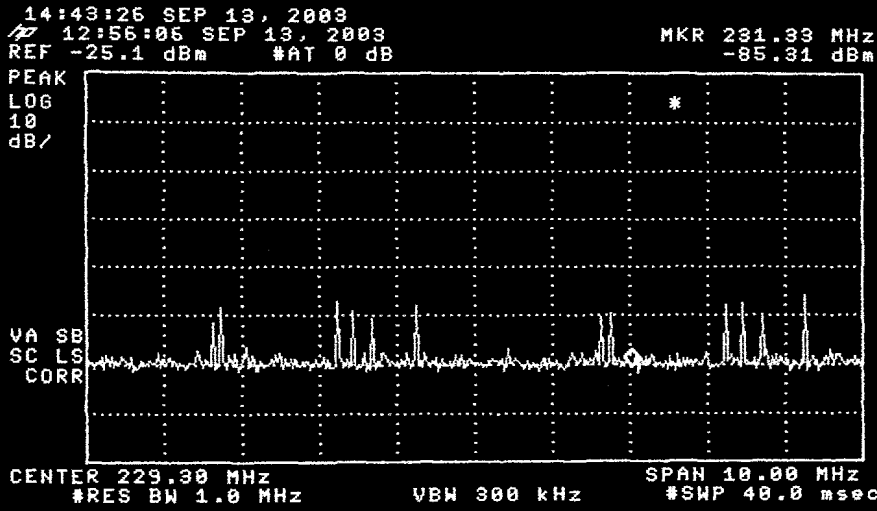
CENTER 130.000 MHz SPAN 0 Hz
 #RES BW 1.0 MHz #VBW 1 MHz #SWP 21.0 msec

(11)

09-04-08 GS + ^ARayhole

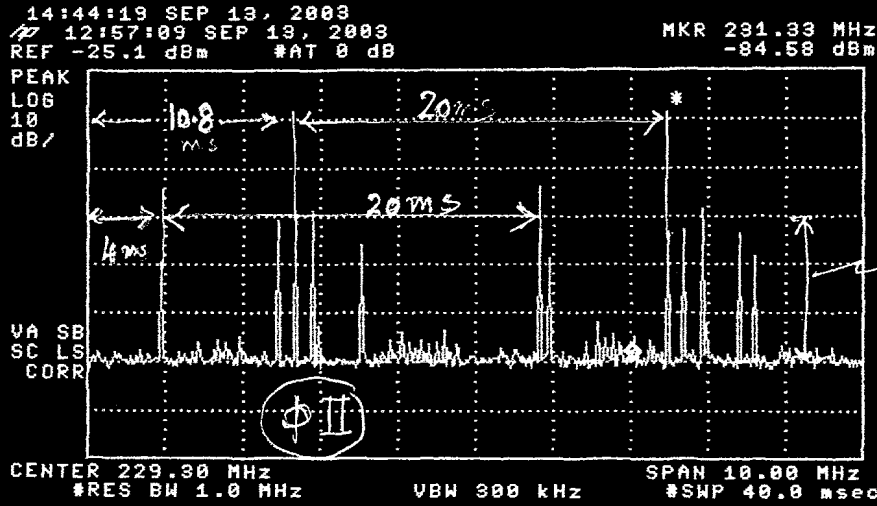
Powerline RFI MEAS-

Fig/5/6-4

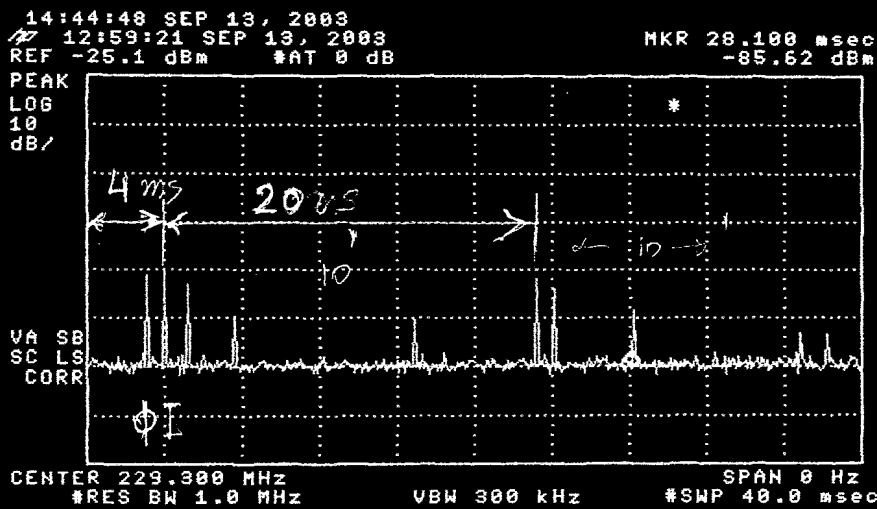


13 Sept 2003
 Antenna?

N



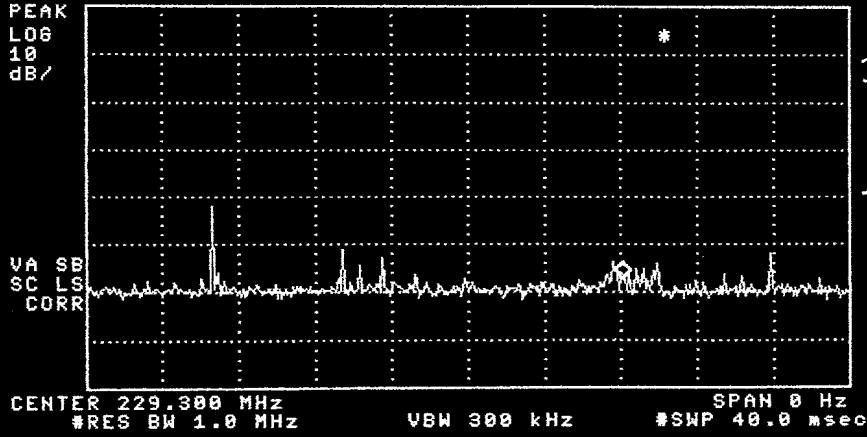
~30 dB
 E
 (phi II)
 phi I



~18 dB
 S
 (phi I)

Fig 5/6-5

13:00:29 SEP 13, 2003 MKR 28.100 msec
 REF -25.1 dBm #AT 0 dB -82.45 dBm

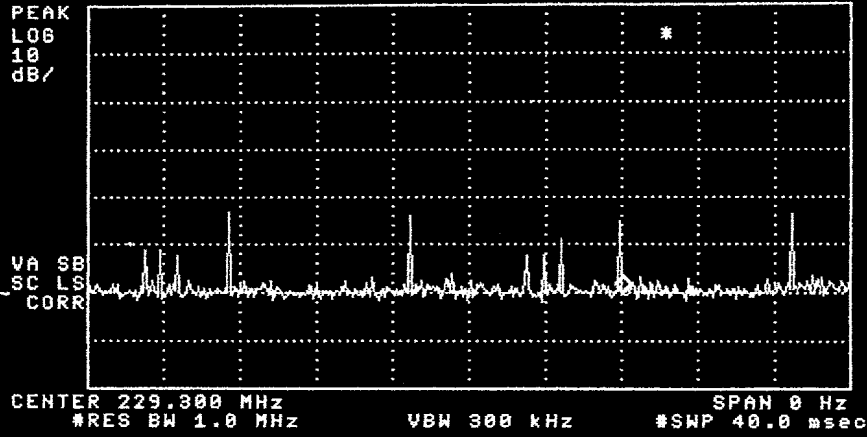


$f = 230 \text{ MHz}$
 $\text{RBW} = 1 \text{ MHz}$

W

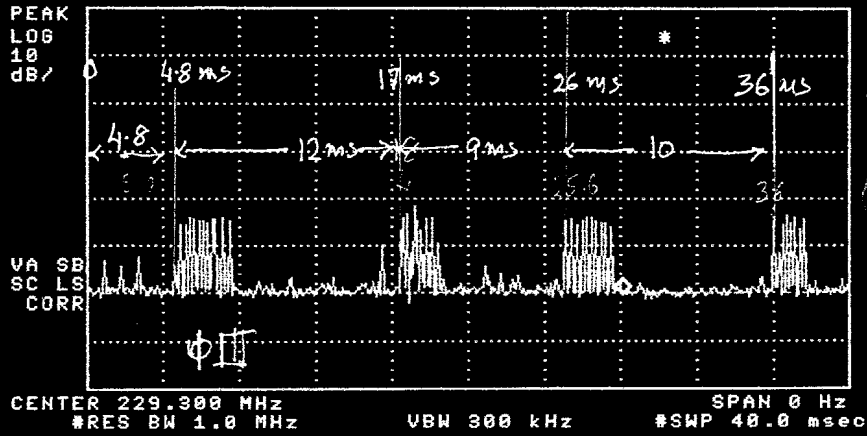
Antenna ?
 OBS - ?

14:45:45 SEP 13, 2003 MKR 28.100 msec
 13:01:11 SEP 13, 2003 REF -25.1 dBm #AT 0 dB -85.04 dBm



N

14:46:10 SEP 13, 2003 MKR 28.100 msec
 13:01:50 SEP 13, 2003 REF -25.1 dBm #AT 0 dB -85.35 dBm



$\sim 15 \text{ dB}$
 $\Phi \text{ III}$

Fig 5/6-5

Table I; Measured values of Electrical-strength of Radio Noise of HT PowerLine :Derived values of Flux Density dBW/m²/Hz at 75 and 150 MHz

Sr.	Reference	E dB/μV/m/Δf F=75 Mhz	EdB/μV/m/120kHz f =75 MHz rms, 200 ft.	S dBW/m ² /Hz f = 75 MHz rms 200 ft.	S dBW/m ² /Hz f = 150 MHz rms 200 ft.
1	Thompson,1984 Fig.S3-4 110 kV	18.5 (quasi-peak) Δf = 120 kHz 200 ft.away	8.5	-188.1	-194.1
2	Nelson, 1980 132 kV Aust. Standard	34 (rms) under the line Δf = 120 kHz	14	-182.6	-188.6
3	Pakala et al. 1967 Fig.S2-2 46 kV line (afterfixed)	60 (peak) 90 ft. away Δf = 1 MHz	25	-171.6	-177.6
4	Pakala et al. 1967 Fig. S2-3 4.6 kV	51±12 (peak) 50 ft. away Δf = 1 MHz	12	-184.6	-190.6
5	Pakala et al. 1967 Fig. S3-1 244 kV	51 ± 14 (peak) 200 ft. away Δf = 1 MHz	22	-174.6	-180.6
6	Pakala et al. 1971 Fig. S3-2 244,345,525,735kV	40 ± 14 (peak) 200 ft. away Δf = 1 MHz	11	-185.6	-191.6
7	Bridges et al. 1970 Fig. S3-3 12 kV vales	Fa = + 18 db above k x 290K 50 ft. away			-196
8	GMRT see Section 7	estimated for 200 MHz, 200 ft. away from 11 kV lines.			-180

NOTES: Based on Pakala et al. 1971 and Thompson 1984 (ref. note Chartier) we have considered RMS -peak = -20 dB; RMS - quasi-peak = -10 dB; 150 MHz- 75 MHz = - 6 dB; used Fig. S3-4 for correcting for distances and 10 log (120 kHz/1MHz) = -9.2 dB.

LOCATION OF RADIO FREQUENCY INTERFERENCE USING GMRT

S. Pathak⁽¹⁾, G. Swarup⁽²⁾, A. Chatterjee⁽³⁾, V. Kale⁽⁴⁾

⁽¹⁾ National Center of Radio Astrophysics, TIFR, Pune, 411007, India. Email: sspathak@sasken.com,

⁽²⁾ As (1) above, but Email: swarup@ncra.tifr.res.in, ⁽³⁾ As (1) above, but Email:

canirban@ncra.tifr.res.in, ⁽⁴⁾ As (1) above, but Email: vishal.kale@waveletgroup.com

ABSTRACT

With the increasing level of Radio Frequency Interference (RFI) in the VHF and UHF bands, it has become important to locate sources of harmful spurious emissions of authorized as well as that from malfunctioning and unauthorized transmitters using phased arrays. We have developed a method for the purpose using existing facilities of the Giant Metrewave Radio Telescope (GMRT) that consists of 30 parabolic dishes of 45-meter diameter each. The dishes are spread over a region of about 25 kilometer. For the present, we have used only 12 antennas of the central array located in a region of about 1 km x 1 km in extent. The primary feeds of the GMRT antennas placed near the focus have a 3dB HPFW of about 60 degrees. We rotate these feeds towards the horizon in specified directions. The voltage signals received by the feeds are cross-correlated using the electronic system of GMRT. The instrumental phase errors are calibrated by transmitting a signal from a signal generator located at a known position with respect to the array of GMRT. Procedure for data reduction and search for the location of an unknown transmitter and preliminary results are described in this paper. Our preliminary measurements show that it is possible to locate position of the unknown transmitter to an accuracy of less than 100 meter for distances of about 5 kilometer in a computer search time of about 100 s. It should be possible to extend the size of the array and use parallel processing computer for searching and locating RFI to much larger distances. The method developed may have wider applications in other communication systems.

1. INTRODUCTION

A radio telescope is typically about 50 or 60 db more sensitive than a communication receiver. For satisfactory operation of a radio telescope, several bands have been protected for radio astronomy observations by the national and international authorities. The Government of India has allocated RF bands near 151-153 MHz, 230-234 MHz, 322-328.6, 608-614 MHz and 1400-1427 MHz for radio astronomy observations using GMRT for which bands no transmitters are allowed up to a distance of several hundred km. However, GMRT observations indicate that there takes place considerable RFI from spurious transmitters in some of the GMRT bands by TV boosters, malfunctioning cable transmissions in nearby region of GMRT and also other unauthorized transmitters located far away. Radio direction finding equipment can find direction of some of these transmitters but with the increasing level of Radio Frequency Interference (RFI) in the VHF and UHF bands, it is become important to locate sources of out-of-band spurious emissions of authorized, malfunctioning as well as unauthorized transmitters using phased arrays. A suitable system for location of such unauthorized or mal-functioning transmitters using phased arrays is also likely to be of interest to many other agencies. In Section 2, we describe theoretical aspects of a procedure developed by us for locating the source of a transmitter whose position was unknown. In Sections 3 and 4, GMRT system in brief, preliminary observations, data analysis, search procedure and results are described. Conclusions are given in Section 5.

2. THEORETICAL CONSIDERATIONS

By multiplying voltages received by all the pairs of the GMRT antennas, we get correlated voltages, $V_j V_k^* = V_j V_k e^{i\Phi_{jk}} + \epsilon_n$, where $V_{jk} = |V_j| |V_k|$, $\Phi_{jk} = (\Phi_j - \Phi_k)$, where $V_j V_k^*$ is the complex products of the voltages received by the jth and kth antennas (j and k runs from 1 to N for the case of N antennas with a total of $N(N-1)/2$ products, and ϵ_n is the receiver noise $= |\epsilon_n| e^{i\Phi_n}$. Let us first consider the case for which the voltage gains caused by the electronics system, called hereafter the instrumental gains, are calibrated and corrected. Receiver or other sources of noise are also not considered for the present.

In order to locate the position of the source of RFI, we require to calculate path lengths d_{g_j} and d_{g_k} from each of the grid points of a search area to all of the j th and k th antennas of the GMRT (Fig.1), the coordinates g being geodetic latitude, longitude and heights of the M 3-dimensional grid points of the search area (Fig.2) and similarly for the coordinates of the j th and k th antennas. GMRT scientists have made accurate determination of the geocentric coordinates of the GMRT antennas using astronomical observations. We have converted these to geodetic coordinates of the GPS system. Thereafter, we calculate corresponding phase differences for each of the grid points to the GMRT antennas, $\phi_{g_j k} = (\phi_{g_j} - \phi_{g_k}) = [2\pi \{ (d_{g_j} - d_{g_k}) / \lambda \} - n]$, where n is an integer. We then subtract these calculated phase differences from the *measured phase values* of the voltage signal from the unknown transmitter, as received by the j th and k th antennas. Assuming that the amplitude of the voltages received by each antennas are equal, say V_0 , we then determine a vector sum, $V_{g_sum}^2$ of all the correlated voltages, $V_{g_j} V_{g_k}^*$, corrected for the corresponding phase differences.

$$V_{g_sum}^2 = \sum_{j=k=1}^{j=k=N} V_{gjk} V_{gjk}^*, \text{ such that } 1 \leq j \leq k \leq N, \text{ for each value of } g, \text{ such that } 1 \leq g \leq M, \quad (1)$$

The amplitude of $V_{g_sum}^2$ is given by,

$$\text{Amp}(V_{g_sum}^2) = \left[\sum_{j=k=1}^{j=k=N} V_0^2 \cos(\phi_{j_k} - \phi_{g_j k}) \right]^2 + \left[\sum_{j=k=1}^{j=k=N} V_0^2 \sin(\phi_{j_k} - \phi_{g_j k}) \right]^2, \quad (2)$$

The value of the phase of the $V_{g_sum}^2$ is given by

$$\Phi(V_{g_sum}^2) = \tan^{-1} \left[\frac{\sum_{j=k=1}^{j=k=N} (\sin(\phi_{j_k} - \phi_{g_j k}))}{\sum_{j=k=1}^{j=k=N} \cos(\phi_{j_k} - \phi_{g_j k})} \right]. \quad (3)$$

The calculated position of the transmitter producing RFI corresponds to the coordinates of the g_{th} point for which the value of the $\text{Amp}(V_{g_sum}^2)$ is maximum and value of the phase $\Phi(V_{g_sum}^2)$ has relatively a low values.

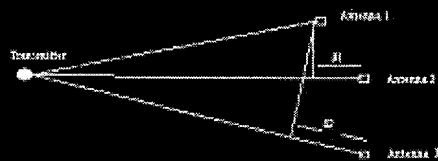


Fig. 1. Determination of path delay between the calibrating transmitter and the GMRT Array.

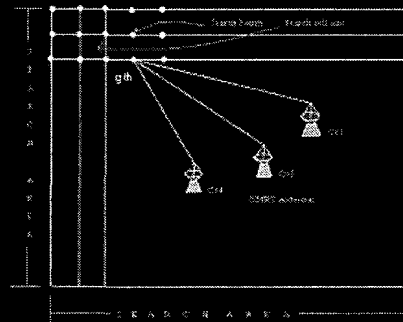


Fig. 2. Three-dimensional search space from g_{th} point to GMRT antennas.

3. COMPUTER SIMULATIONS

In order to test our concepts, computer simulations were carried out using parameters of the GMRT central array, considering a source of RFI located 10 km away and then calculating value of the peak response of the maximum (main lobe) and of secondary maxima with and without phase errors of about ± 50 degrees. It was shown that the main lobe had appreciably higher value than that of secondary maxima. It's half power width was about 50 m [1].

4. GMRT OBSERVATIONS AND DATA ANALYSIS

GMRT consists of 30 fully steerable parabolic dishes, each of 45 m diameter, located in a region of about 25 km in extent [2]. Twelve antennas are located in a central array of about 1 km x 1 km in extent and other 18 antennas are placed in three Y-shaped arms, each 12 km in length. The GMRT operates as an Earth Synthesis Radio Telescope and produces antenna beam of the GMRT array for celestial observations with relatively low side-lobes in a typical observing period of several hours. The signals received by each of the 45 m dishes are amplified, converted to IF signals, transmitted on optical fibers and brought to a central receiver room where all the received voltage signals are cross multiplied using a complex correlator and finally recorded in a computer system.

In order to test the method described in Section 2 and to develop a suitable search procedure, preliminary observations were made at the GMRT site in Feb. 2004, software developed and then again on March 10 2004 as described here. For these observations we used only 12 antennas of the central array of the GMRT located in a region of about 1 km x 1 km in extent. The primary feeds of the GMRT antennas that are placed near the focus of each antenna have a gain of about 8 dB and 3dB HPBW beam-width of about 60 degrees. We rotated these feeds towards the horizon in a western direction. As described above, the voltage signals received by the feeds are cross-correlated using the electronic system of GMRT. The phase errors of the electronics system, called instrumental phase errors, were calibrated by transmitting a signal from a signal generator located at a position about 7 km away from the array of GMRT using a log-periodic antenna facing the GMRT array.

The location of the calibrating signal generator was measured using a GPS receiver. A second signal generator was placed at a distance of about 5 km from the GMRT towards northwest direction from the GMRT central array and whose position was considered as "unknown" during the data reduction. A search procedure was developed as described below and allowed us to determine the position of the unknown transmitter. Its position was later determined using a GPS receiver and differences between the results of search procedure and GPS measurements were tabulated.

The GMRT correlator and computer system provides a 'LTA' file giving sequential complex values of correlation between various antennas typically every 16 seconds. The LTA file also contains various parameters of the GMRT antennas, such as time of observation, elevation and azimuth or hour angle of various antennas.

Using the Astronomical Image Processing System (AIPS) software that has been developed by the National Radio Astronomy Observatory (NRAO), USA, the data was converted to a standard FITS format. The data was flagged using the VLOT task. Accurate frequency of signals received from the calibrating and unknown transmitter was determined using the task POSSM. Amplitude and phases of the calibrating transmitter were then determined using the CALIB task, with respect to a selected reference antenna. Path lengths between the measured positions of the calibrating transmitter and GMRT antennas were calculated. The corresponding phase values for these path lengths were then subtracted from the output of the SN table created by the CALIB task, which provided us values of the *instrumental error* ϕ_e of the electronic system of each antenna of GMRT. From these values we then constructed a *matrix table* giving $\phi_{e_j k}$ for all the antennas.

The phase matrix $\phi_{u_j k}$ for the unknown transmitter was obtained using the LISTR task. From these phase values we subtracted the matrix $\phi_{e_j k}$, which provided phase matrix $\phi'_{j k}$ of the voltage received from the unknown transmitter and corrected for instrumental errors. In order to determine the location of unknown transmitter, a search procedure was developed in which we divided a selected search area into 3-dimensional grid points, g (Fig. 2). We then calculate phase values, $\phi_{g_j k}$ as described in Section 2 and finally amplitude and phase responses using Eqs. (2) and (3) for each of the g_{th} grid points. The maximum value of the amplitude and minimum value of phase of $V^2_{g_{sum}}$ for a particular grid point determines the location of the unknown transmitter.

We have so far not discussed various parameters such as phase errors due to receiver noise and multi-path propagation. We also expect to get secondary maxima due to the expected 'side lobes' of the GMRT array

towards relatively nearby locations in the search area. We therefore made contour plots of $\text{Amp}(V_{g_sum}^2)$ (Fig. 3) and also of $\Phi(V_{g_sum}^2)$. For observations made on 10th March 2004, 12 antennas were used and hence we expect a maximum value of $N \times (N-1)/2 = 12 \times 11 / 2 = 66$. Our search routine give us a maximum value of 40 in a search period of 73 sec over a region of about 1.5km x 1.5km and height variations of about 150m. The position of the peak value of the amplitude of $V_{g_sum}^2$ provided us coordinates of the unknown transmitter. The differences between these coordinates and GPS positions, (which may be considered errors in determination of location of the unknown transmitter), were found to be as follows: Δ latitude = 64 m, Δ longitude = 2 m, Δ height = 89 m. There were several 'side-lobes' as seen in Fig. 3 but their phases had large values.

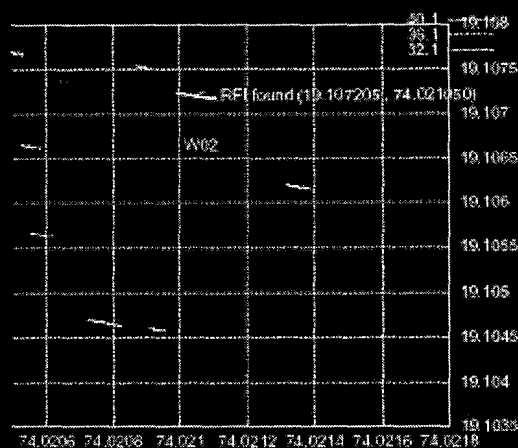


Fig. 3. RFI Search plot giving location of the unknown transmitter at W02.

4. DISCUSSIONS AND CONCLUSION

Our preliminary observation and search procedure developed show that a 2-dimensional array of limited number of antennas distributed over an area of about 1 km x 1 km can locate sources of RFI up to several km away from the GMRT array, by using only the primary feeds of the GMRT 45m dishes which have a gain of only about 8 dB. One of our motivations for the above work was to locate the source of RFI observed at GMRT at 229.4 MHz during a search for the expected neutral hydrogen absorption from the farthest known radio galaxy in the Universe at a redshift of 5.1. Our observations indicated that the source of RFI could be from the city of Pune that is about 60 km away from the GMRT. Considerable more work needs to be done by using more antennas of the GMRT for locating sources of RFI up to tens of km away. For search over a large region, one may use better algorithms including parallel processing algorithms. Since GMRT antennas can be rotated only from 17 degrees to

90 degrees from the horizon, it is not possible to use the full 45 m dishes for detecting and locating the sources of RFI. For finding sources of RFI in the region of about 15 to 20 km around the central array of GMRT other methods are being tried by the GMRT group and need to be further explored. The method developed is likely to be useful for locating sources of RFI much further away. It may also be applicable for the general problem of locating malfunctioning or unauthorized transmissions affecting other communication systems near cities by setting up special phased arrays.

5. ACKNOWLEDGEMENTS

The project was carried out by S.P. and V.K., as their project for the M. Tech. degree of the engineering university at Lonare and by A.C. as a project of the M.Sc. (Computer Science) of the University of Pune, under the guidance of G.S.; S.P., V.K. and A.C. thank their Heads of Depts. for providing encouragement. We also thank the staff of GMRT for valuable help in making observations.

6. REFERENCES

- [1] A.Chatterjee, "Computer Simulation for locating sources of RFI", Internal Report, NCRA-TIFR, 2005.
- [2] G. Swarup, S.Ananthkrishnan, V.K. Kapahi, A.P. Rao, C.R. Subrahmanya and V.K. Kulkarni, "The Giant Metrewave Radio Telescope," *Current Science*, vol. 60, pp. 95-105, January 1991).

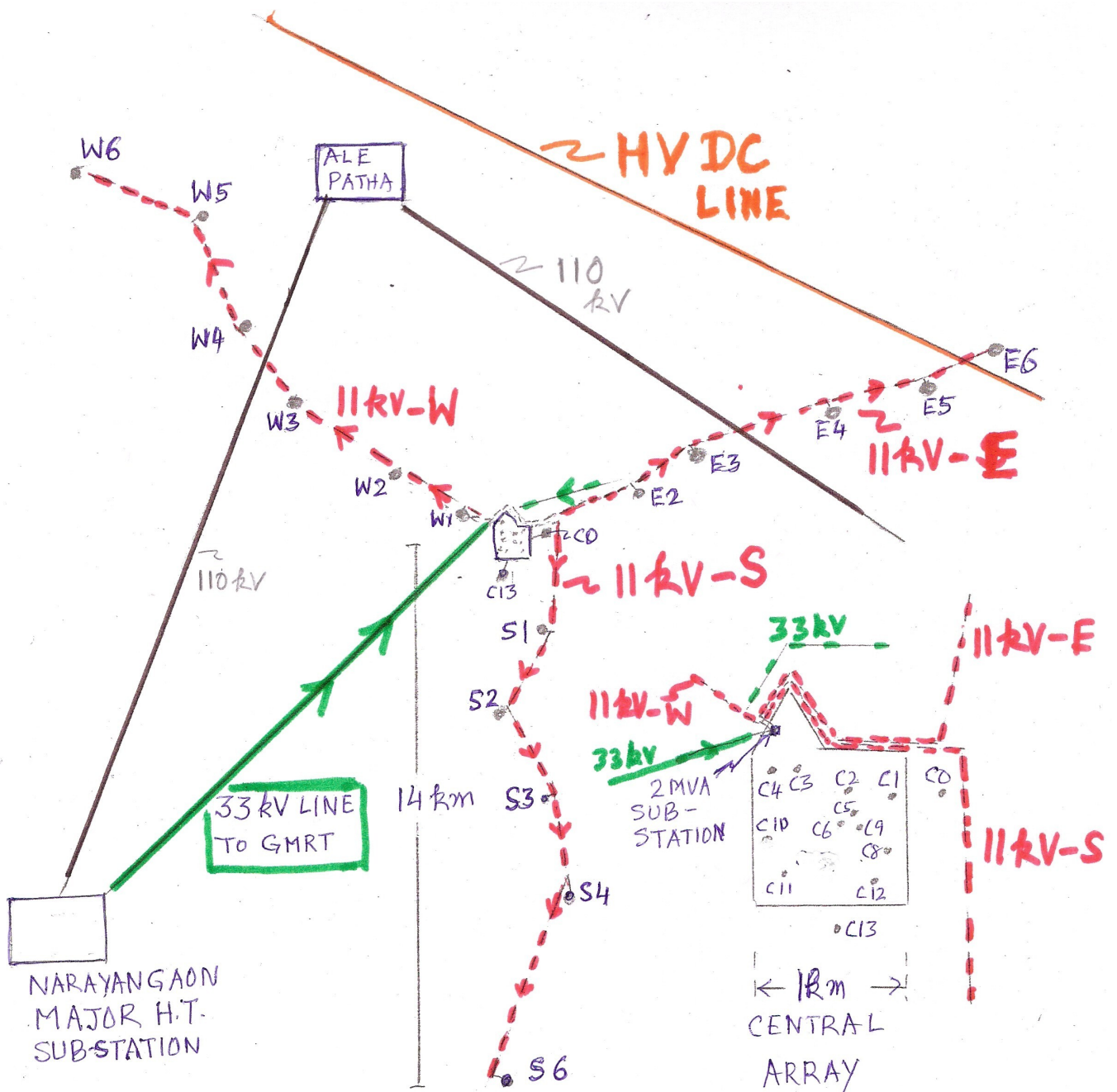


[FIG. S1-1] LAY OUT OF HIGH TENSION (H.T.) ELECTRICAL LINES SUPPLYING POWER TO GMRT

(A 33 kV line from Narayangaon sub-station supplies power to a 2 MVA sub-station at N-W corner of GMRT. From the 2 MVA station, one line goes to a transformer supplying power to the CENTRAL ARRAY & 3 lines to the E, S & W arrays)

G. SWARUP 12 July 2008

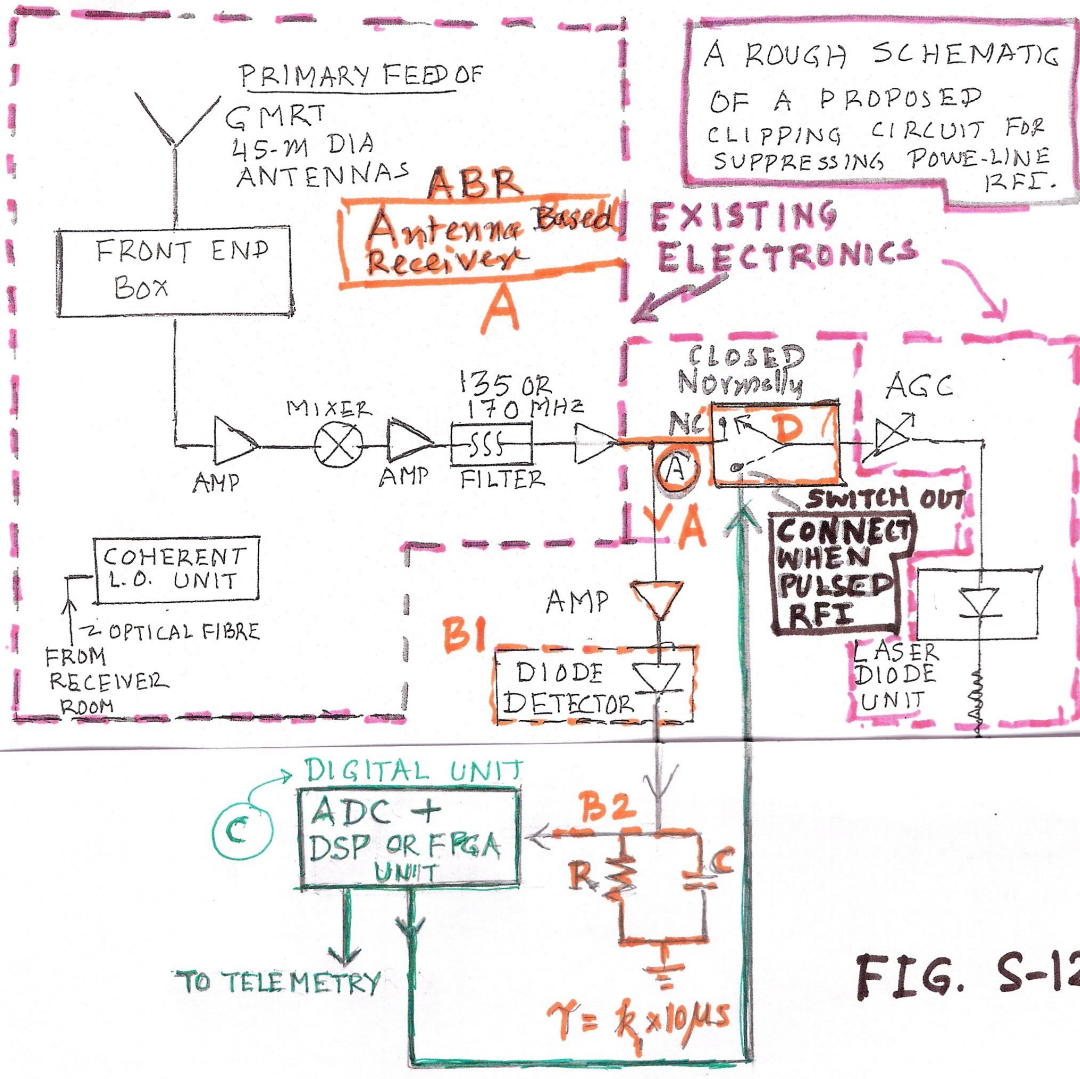
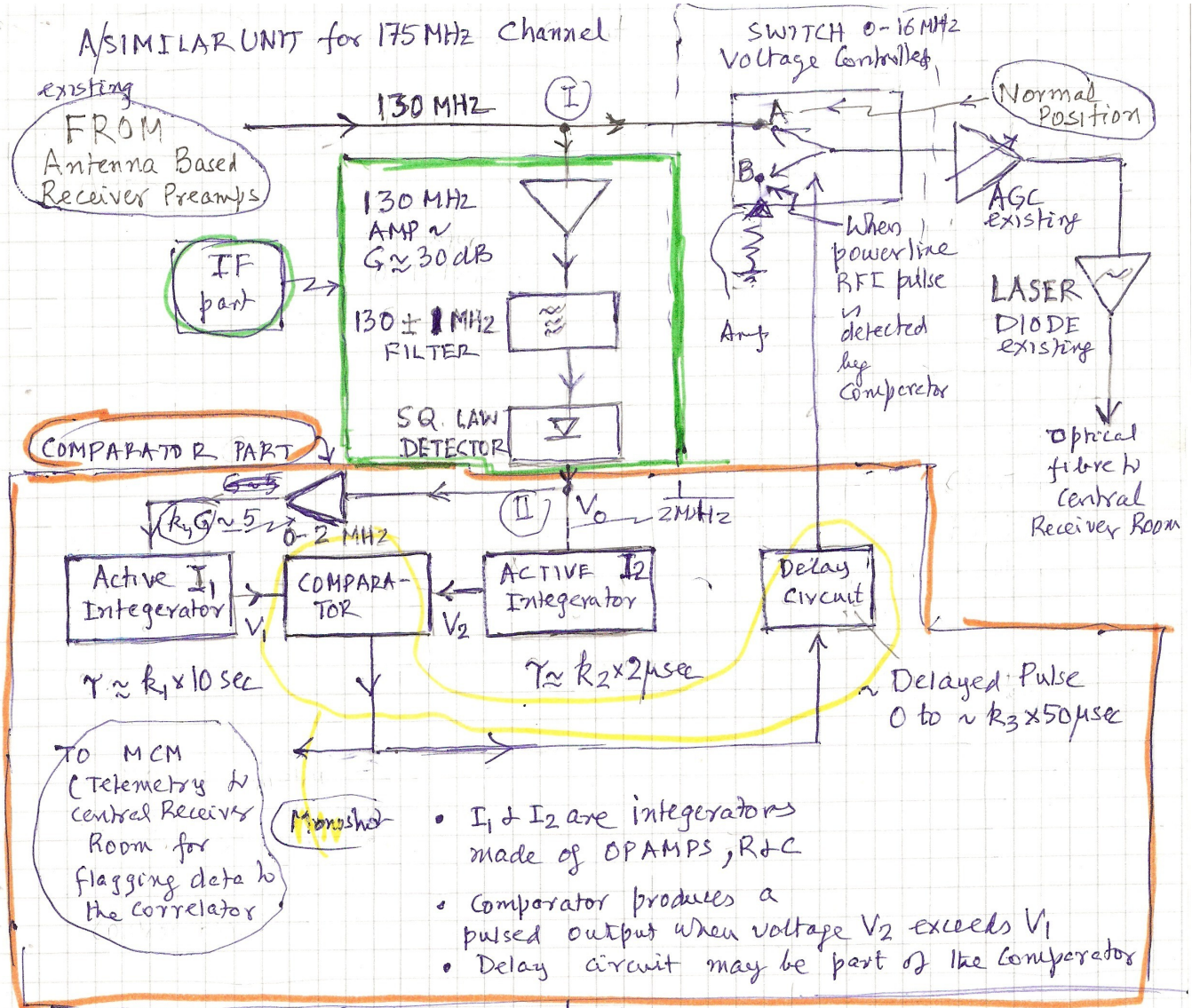


FIG. S-12-1

DSP OR DIGITAL UNIT WITH FOLLOWING LOGIC

1. The Output **A** of 135 (or 170 MHz) amplifier is connected to an integrator (**B₁+B₂**) giving mean value of received power P_1 with a time constant of about 10 to 20 μs (k_1 to be determined experimentally)
- $P_1 \rightarrow$ 2. The output of the integrator $(\frac{E}{T} = P_1)$ is applied to an ADC unit followed by a DSP or FPGA unit (Digital Unit) **C**.
- $P_2 \rightarrow$ 3. Digital unit is to be programmed to integrate the incoming ~~volt~~ power to a time constant of $\sim k_2 \times 10$ seconds (k_2 to be determined experimentally) $= P_2$.
If P_1 exceeds P_2 , the digital unit, **C**, sends signal to switch **D** to disconnect the ABR output that is normally connected to AGC. It sends signal to Central Receiver Room through telemetry

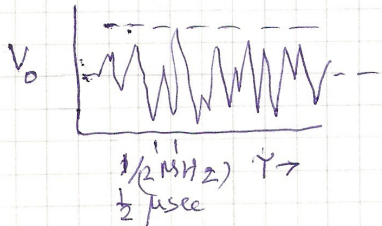


A simplified Block diagram to describe the ~~pub RFI~~ Powerline-pulsed RFI suppression circuit using a **Comparator** instead of DSP

FIG. 5-12-2

(See Annexure)

consider output of sq. law detector for gaussian random noise



- V_o varies from a mean value \bar{V}_o to $\bar{V}_o \pm 3$ rms (poisson distribution) \rightarrow RMS $\approx \bar{V}_o$ for poisson dist
- when ~~pub~~ powerline-pulsed RFI takes place, it exceeds ~ 3 rms, comparator produces a pulse output from $t_1 = 0$ to $t_1 + k_3 \times 50$ μ sec

k_1, k_2, k_3 to be determined experimentally

G. Swamy
[7/10] 8 1:19 PM

(p. 52)